POLITECNICO DI TORINO

Master Degree in Biomedical Engineering

Master Degree Thesis

Ultrasound scanning of inferior vena cava to study the hydration condition during sport

Supervisor

Prof. Luca Mesin

Co-supervisor

Ing. Piero Policastro

Candidate

Eleonora Canale

2023

Abstract

Water is essential for our body: more than 60% of our weight is made up of liquids. The analysis of fluid loss during sports performance is crucial for an athlete, as intense sweating can cause dehydration. Dehydration can lead to worsening of sports performance, cardiovascular fatigue and, if prolonged and in extreme situations, even hyperthermia, failure of the gastrointestinal system, heat cramps and death. Fluid balance, i.e. the optimal ratio between fluid intake and loss, is critical to athlete performance and safety during exercise, especially in extreme environmental conditions such as high-temperature environments. Being able to perform a fluid loss analysis in a short time and with precision is certainly useful to optimize training and physiological recovery. The aim of this master's thesis is therefore to investigate the fluid dynamic response of the athlete after an effort, noting its effects on the IVC. Currently, methods are used that require long processing times and, consequently, also lengthen the time to know the results, making timely intervention impossible. The ultrasound analysis of the inferior vena cava (IVC), on the other hand, is immediate and allows to verify in real time the volume status of the sports subject, providing an estimate of the hydration status. The main objective of the project is precisely to study the level of hydration of athletes during sports activities and during recovery, to monitor them and improve their performance through real-time control of the diameter of the IVC, using a portable ultrasound probe and a segmentation software owned by Viper s.r.l. To this end, some candidates were subjected to sweating activity. In detail, the dataset is composed of 21 subjects, 9 women and 12 men, and contains healthy subjects differentiated into sportsmen (14) and non-athletes (7), with an age of 24 +/- 2 years and a weight of 70.3 +/- 11.8 kg. The test protocol provided for subjecting candidates to a sporting activity, i.e. 4 sloping walks on a treadmill lasting 10 minutes each, with slope and speed parameters varying according to the amount of weight lost. During the activity, a POLAR band was worn for ECG monitoring and ultrasound scans of the IVC were performed to observe the variation in the diameter of the IVC, assuming a reduction during the activity. At the end of the acquisition phase and after obtaining the average diameter in the different frames of the ultrasound video, three parameters were calculated that indicate the collapsibility of the IVC: caval index (CI), respiratory caval index (RCI) and cardiac caval index (CCI). By correlating these parameters and segmented diameters with initial patient data by means of statistical tests (two-sample t-test, one-way ANOVA, multi-way ANOVA), any significant differences in the dataset were evaluated, but were not highlighted. However, the initial assumption on the diameter trend was respected. During exercise, a gradual reduction in the diameter

of the veins was noted, while an increase was observed during hydration. The demonstration of these trends was obtained by interpolation between values using linear regression.

Table of Contents

List of Tables

List of Figures

Chapter 1

Introduction

One of the main vessels of the circulatory system is the inferior vena cava (IVC). It is the largest vein of the human body, located at the posterior abdominal wall. The IVC function is to carry the reflux blood from the inferior body part (abdominopelvic region and lower limbs) to the heart. Its elastic walls make the vessel size sensitive to pressure changes produced during cardiac and respiratory activity. Changes in IVC transmural pressure are observed during the respiratory cycle; in fact, during expiration the IVC exhibits its maximum size, while during inspiration we can observe a slight reduction in size, this due to a lowering on intrathoracic pressure. Instead, during positive pressure ventilation (mechanical ventilation) we can observed an opposite behaviour with an increase in size during inspiration and a reduction during expiration. During the cardiac cycle, the size of the IVC increases during atrial contraction and decreases before atrial systole. Pathological conditions and manoeuvre that alters the pressure and bloom volume in the abdominal compartment causes variations on the IVC size. For these reasons a close observation and study of the changes in size of this vein and its pulsatility is of great interest in medicine. IVC calibre assessment can be used to estimate right atrial pressure (RAP), that normally is estimated using an invasive measurement, and volemic status by means of pulsatility indices such as caval index (CI), collapsibility index and distensibility index. These indexes are calculated using the different diameter observed in respiratory cycle. In particular, the ratio of the maximum diameter to the minimum diameter is exploited for the calculation as follow:

$$\frac{D_{max} - D_{min}}{D_{max}} \tag{1.1}$$

However, the analysis of the pulsatility of this vein is particularly complex because its cross-section is often non-circular and not constant, and it is a very compliant vessel that exhibits anisotropic deformation during spontaneous breathing and fluid challenges. There are different imaging modalities available in cardiology,

but echocardiography is definitely the most useful when it comes to hemodynamic analysis. The main types of ultrasounds used to analyse the IVC are the M-mode and B-mode. M-mode works along a fixed direction and on screen is shown a section of the vein, from which the diameter can be estimated. However, the analysis may be inaccurate due to variations over time of the diameter of the vessel, caused by its movements, and due to the difficulties in proper alignment perpendicularly to the vein. On the other hand, B-mode allows complete visualization of the IVC in both planes, transverse and longitudinal. But in this case the choice of the vessel section is highly operator dependent and therefore the measurement becomes potentially inaccurate. In addition, the results of these modalities are not much reproducible because is up to the operator the decision of the moment in which the measurements should be taken. A start up called Vein Image Processing for Edge Rendering (VIPER) has developed new software that can detect the inferior vena cava and follow its movements in both the transverse and longitudinal planes to go beyond these limits. The goal of the software is to provide repeatable and accurate measurements to assist clinicians in making diagnosis and treatment decisions. The objective of this thesis is to observe the effects of athletes' sweating on the inferior vena cava using the latest release of the VIPER software. Usually in the athletic setting, hydration status is estimated by monitoring the weight and the urine concentration, but these methods are slow and impractical because sometimes a rapid and accurate assessment is needed during professional competitions. Hypothesis is that IVC diameter measurements, in particular caval index and diameter variation itself, are related to percent weight loss. The first chapters will focus on a description of the anatomy of the cardiovascular and respiratory systems. next will be a description of the principles of ultrasound and ultrasonography and an explanation of dehydration and its implications on health and IVC. Finally, the methods used, tests performed, and results obtained will be discussed.

Chapter 2

Cardiovascular system

The circulatory system is formed by a network of channels of different calibre, the vessels, in which circulate the blood and the lymph. A distinction is therefore made between a blood circulatory system and a lymphatic circulatory system. The first is the one we are interested in, and it is composed of the heart, arteries, capillaries, and veins. This system is a closed circuit in which the blood is pushed from the heart into vessels with a centrifugal course, the arteries, which, branching out and gradually reducing in calibre, resolve themselves, inside the organs, into very thin vessels, the capillaries [1]. From these are formed the veins, with a centripetal course, which bring back the blood to the heart. The heart is divided into right heart and

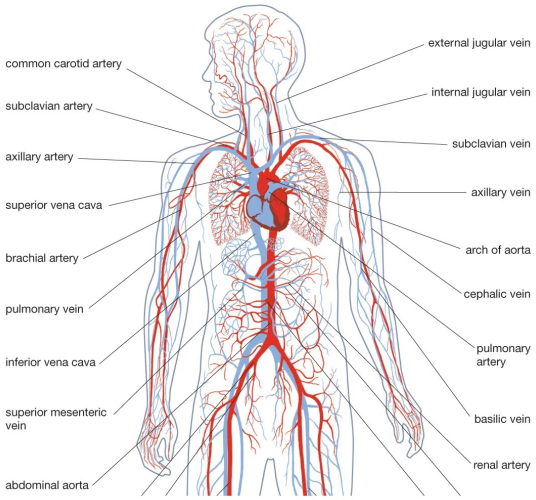

Figure 2.1: *The figure shows the circulatory system and its major vessels.*

left heart, two independent halves, and each of these are formed by a superior cavity, the atrium, and an inferior cavity, the ventricle. Atria and ventricles communicate

through an atrioventricular valve. The two atria are headed by veins, and from each ventricle, through semi-lunar valves, a large arterial vessel departs. The blood circulatory system is then divided into great circulation (general circulation), that origins from the left side of the heart, and small circulation (pulmonary circulation), that origins from the right side of the heart. The great circulation begins in the left ventricle with the aorta, an arterial trunk. The arterial blood, as it passes through the capillary networks that join the arteries to the veins, supplies metabolites and oxygen and is loaded with catabolites and carbon dioxide [1]. In this way, the blood changes from arterial to venous, with a darker colour. The venous blood, via venous branches, the most important of which are the hollow veins, superior and inferior, returns to the heart. The venous trunks flow into the right atrium from which then the blood passes into the right ventricle. The small circulation begins in this ventricle with the pulmonary trunk, which bifurcates and carries venous blood to the two lungs. These branches arrive at a capillary network located on the surface of the pulmonary alveoli walls. The venous blood, passing through this network, gives up carbon dioxide to the atmospheric air and takes in oxygen; having thus become arterial, the blood returns to the heart through the pulmonary veins, which carry it to the left atrium [1]. Then it passes into the left ventricle and the circle start again. Blood pressure regulates blood flow and is therefore essential for maintaining the body's homeostasis [2]. The mean systemic pressure (MSP) is the pressure that the blood has within the entire cardiovascular system with a stopped heart. Two conditions are necessary to the heart to permit blood circulation:

- A MSP bigger than zero;
- Stretchable vessels.

The first condition is always verified because the system contains an excess of blood volume, and the value of the MSP is about 7 mmHg [1]. The heart is a volume and pressure divider because, by pulsating, it moves blood from the venous to the arterial district, decreasing the pressure in the former and increasing it in the latter. In the left ventricle, the pressure has systolic-diastolic fluctuations from 0 to 120 mmHg. In the arteries, the oscillations have a reduced amplitude because their diastolic value is 70-80 mmHg due to the presence of the aortic valve and peripheral resistances [3]. Instead, due to the lower pre- and post-capillary resistances, in pulmonary circulation the pressure values are lower than in the general circulation. These resistances low values also allow the pressure to remain pulsatile in the alveolar capillaries. Some important parameters for defining blood pressure values are: cardiac output (CO) defined as the amount of blood pumped by the heart per minute, peripheral resistance (PR) which is the total resistance that opposes blood flow, and mean arterial pressure (MAP) which turns out to be the average

between diastolic and systolic pressure in the aorta. The MAP is proportional to the product between the first two values according to the following relationship:

$$CO = MAP/PR \tag{2.1}$$

Each vessel can be assigned its own pressure, called transmural pressure (P_{tm}, which is the difference between pressure in and out of it, and its changes cause variations in the very size of veins and arteries. The relation between vascular size and P_{tm} is generally represented by a non-linear volume-pressure curve (figure2.2), according to which vascular size increases as transmural pressure increases [2]. In arteries, transmural pressure is influenced by the pulsatile nature of the heart pump and peripheral resistances, whereas in veins, which are characterized by lower internal pressure, it is influenced by changes in external pressure. Vessel compliance (C) is defined by the slope of the volume-pressure curve:

$$C = \frac{DV}{DP_{tm}} \tag{2.2}$$

The curve tends to flatten at high P_{tm}. We can therefore observe that a change in

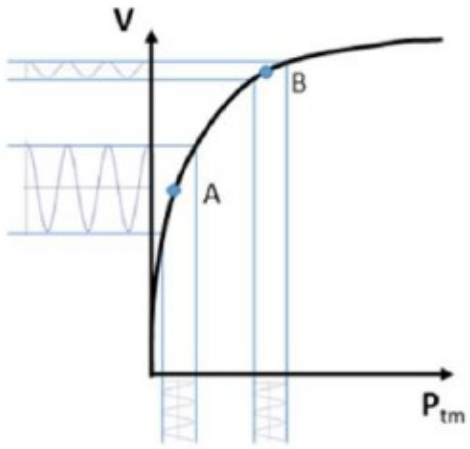

Figure 2.2: *Here is shown the volume-pressure curve. [4]*

P_{tm} will also result in a change in vessel volume. If the mean P_{tm} is high, as in arteries, the vessels size will be larger and the phase changes will be small, but if it turns out to be low we will have larger caliber changes. In other words, when measuring changes in vessel volume in response to given variations in blood pressure, we are assessing the total compliance (C_{tot}), which accounts for the vascular (C_v) and extravascular (C_{ev}) compliances according to the formula:

$$C_{tot} = \frac{1}{\frac{1}{C_v} + \frac{1}{C_{ev}}} \tag{2.3}$$

C_{tot} resulting smaller than C_v [4].

2.1 Structure of arteries and veins

2.1.1 Arteries

Arteries are musculo-membranous conduits lined internally by endothelium. The major arteries are the aorta, from which the arteries of the general circulation are derived, and the pulmonary trunk, which supplies the arteries of the pulmonary circulation. Each artery may give off collateral vessels of a smaller calibre and are often accompanied by one or two veins and one or more nerve trunks; together these formations constitute a vascular bundle. The wall of the arteries consists of three concentric tunics called, from the inside out, intima, media, and adventitia. The media tunica, which is also the thickest, characterises the functional behaviour of the arteries based on its constitution. The media tunica is principally made of muscle tissue in the arteries of small and middle calibre, while it is made of elastic tissue for that of major calibre. So, we can distinguish two types of arteries:

- muscular type: they have contractile walls and can actively vary their lumen regulating the amount of blood flowing to organs;
- elastic type: they have elastic walls and have a passive function in the blood circulation.

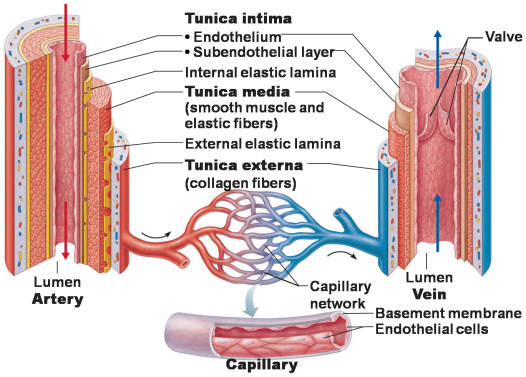

Figure 2.3: *In this figure are shown the different structure of arteries and veins.*

Large-calibre arteries are those with a diameter between 3 cm and 7 mm, medium-calibre arteries those with a diameter between 7 mm and 2.5 mm and small-calibre arteries and arterioles those with a diameter of less than 2.5 mm.

2.1.2 Veins

Veins are membranous ducts, and they originate from the capillary networks of tissues and organs until they converge to form trunks of increasing calibre. They lead the blood returning to the heart from the capillary district to a pressure regime that is considerably lower than that which exists in the arterial tree, a factor of primary importance for their structural characterisation [1]. The main differences between veins and arteries are the following:

- the walls are thinner and less elastic;
- they are easily depressible and dilatable;
- they have valves.

The typical shape of the veins is cylindrical, but when they are empty of blood, they may appear flattened and collapsed. Their number is greater than that of arteries. The overall calibre of the affluent branches is greater than that of the venous trunk that originates from their confluence: the vascular bed is narrowing from the periphery towards the centre and, as a result, the venous current is gaining speed in the direction of the heart [1]. They too, like arteries, are divided into large-, medium- and small-calibre veins. A further distinction is made into superficial and deep veins. The formers are located in the subcutaneous portion, while the latter are found in the muscle interstices and visceral districts. Most veins have valves, pocket-like membranous folds rising from the venous wall with the concavity in the direction of the heart. The distribution of these valves is not regular but correspond to specific functional needs. There are numerous in the districts where the outflow is more difficult, such as in the lower limbs. The walls of the veins, like those of the arteries, are divided into three layers, or tunics: inner (or intima) tunica, media tunica and adventitia (or outer) tunica. However, in the veins this structural schematization is not constantly applicable and often the boundaries between these tunics are not that evident. The elements composing the veins walls are that also typical of the arteries: endothelium, collagen fibre, elastic fibre, and muscular cells. The wall of veins differs from that of arteries mainly due to the greater presence of collagen material, that forms the underlying texture, to the disfavour of the elastic contingent. Furthermore, there are several structural differences between the veins themselves. We can, for example, distinguish receptive-type veins with thin walls and propulsive-type veins with thick walls.

2.1.3 Inferior Vena Cava

All the veins in the subdiaphragmatic part of the body lead to the inferior vena cava that is also the largest vein in the human body. It resides in the abdominal

cavity where it runs vertically to the right of the vertebral column and, for a short distance, in the thoracic cavity where it ends by opening into the right atrium of the heart [1]. It has an average length of 22 cm, of which 18 cm in the abdominal portion, and a calibre of approximately 30 cm. It arises from the union of two common iliac veins at the level of the fibrocartilage between the 4th and 5th lumbar vertebrae. From this point goes up to the right atrium of the heart and along the road it receives numerous affluents. It falls into the group of propulsive-type veins, which are characterised by a thick wall thus constituted:

- the tunica intima consists of the endothelium, a thick subendothelial lamina and sometimes bundles of muscle cells in a longitudinal oblique arrangement;
- the middle tunica is considerably thick and can make up as much as 2/3 of the wall and is made up of collagenous bundles and abundant bundles of muscle cells in a circular or spiral arrangement;
- the adventitia tunica is well developed and consists of collagenous connective tissue containing elastic fibres arranged in a network.

The inferior vena cava is characterized by high compliance, i.e., a good ability to expand elastically under the effect of increasing blood pressure and then shrink by returning the accumulated blood volume under the effect of decreasing blood pressure [2]. As described earlier transmural pressure changes affect vessel size, and the vena cava is no exception. These pressure changes are regularly produced by the cardiac and respiratory cycles and consequently cause ivc movements in the longitudinal and transverse planes during breathing.

Chapter 3

Respiratory system

The cells of the human body require oxygen (O_2) to survive and produce carbon dioxide (CO_2) during aerobic respiration. The respiratory system is the anatomic structure that enables the exchange of gases between the air and the blood, as well as having other functions such as: contribute to the regulation of the blood basic-acid equilibrium, permit phonation, participate to the defence against pathogenic factors and external particles in the airways, supply a way to dissipate humidity and heat, increase the venous return and activate some plasmatic proteins when they pass through the pulmonary circulation [5]. The respiratory system consists of a set of canal-like organs and the lungs in which take place gas exchanges between air and blood. The airways can be divided into superiors and inferiors; nasal and paranasal cavities and the nasal part of the pharynx are part of the first, while the inferior airways consist of the laryngotracheal duct and the bronchi leading to the lungs, within which they are distributed with various order of branches [6]. The airways remain constantly pervious thanks to the bony or cartilaginous skeleton in their walls. This facilitates the passage of air. The walls are lined with mucous membrane, called respiratory mucous membrane, which performs a function of lining the walls, heating (due to its great vascularisation), humidifying and filtering (mucus stops atmospheric dust) the air before it reaches the respiratory area. There are also some specialised traits for olfactory (olfactory mucosa) and phonation (larynx) functions. Numerous cavities are hollowed out in the lungs, the pulmonary alveoli, which have very thin walls and are covered with capillaries, also very thin walled, allowing rapid gas exchange between air and blood. The lungs are thus the organs where the passage of oxygen from the alveolar air to the haemoglobin contained in the red blood cells circulating in the perialveolar capillaries takes place; a reverse pathway, from blood to air, is followed by carbon dioxide, which is eliminated with expiratory air [6]. These formations are the so-called air-blood barrier. The initial part of the respiratory tract is the nose, and it is involved in respiratory and olfactory activities. It is composed of cones and

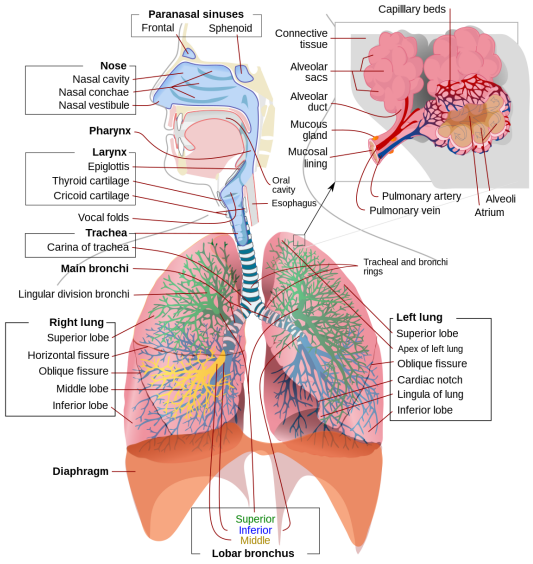

Figure 3.1: *The figure shows the organization of the respiratory system and its anatomy*

cartilage, that forms its external structure, and inside it we can find the anterior parts of the nasal passages, which consist of two long, winding channels covered with mucous membrane that open into the nostrils towards the outside of the body. The larynx takes the form of a hollow triangular pyramid. Besides being the organ par excellence responsible for phonation, it allows the passage of inhaled air (from the nose and mouth into the bronchi) and exhaled air (from the bronchi into the nose and mouth). The communication between the larynx and pharynx, through which this passage of air occurs, is called the laryngeal aditus or upper laryngeal opening and is an ovoid orifice. It is fitted with a closing device that prevents the entry of chewed food (food bolus) from the mouth during swallowing. The larynx actively rises and falls during swallowing, breathing and phonation; it moves passively with the movements of the cervical spine. The trachea connects the larynx with the initial portion of the bronchi, in which it bifurcates at the fifth dorsal vertebra, dividing into the two bronchial trees, right and left. Has the shape of a cylinder flattened posteriorly, about 10-12 cm long and 16-18 mm in diameter [6]. It is made up of 15-20 cartilaginous rings, which keep the lumen of the trachea constantly pervious, connected to each other by fibrous laminae called annular ligaments. They are incomplete posteriorly where the so-called membranous wall of the trachea is located. The trachea is divided into two parts:

- cervical part: about 4 cm long and includes the first 5-6 tracheal rings;

- thoracic part: is the rest of the trachea, surrounded by loose connective tissue.

The bronchi are cylindrical conduits between the bifurcation of the trachea and the bronchioles whose task is to allow and ensure the passage of air from the trachea to the bronchioles and pulmonary alveoli. There are two main bronchi in the human body: the right bronchus and the left bronchus from which arborization originates, most of which is contained in the lungs. The left bronchus has a minor calibre, but a major length of the right bronchus. This is because the right lung is more ventilated as it has more volume and greater breathing capacity. The bronchi are also related to the branches of the pulmonary arteries, the pulmonary veins, the bronchial arteries, and the anterior and posterior bronchial veins. The two main bronchi then branch, reducing their calibre until they reach the level of the terminal bronchioles, that have a diameter of less than 1 mm and even smaller. The two lungs are the organs in which gaseous exchanges (haematous) actually take place and are contained in the pleuropulmonary chambers of the thoracic cavity. The lungs are surrounded by the pleura, a serous membrane made up of two sheets, a visceral one which adheres to the surface of the organ, and a parietal one which covers the surface of the lung lodges. Between the two sheets is the pleural cavity, in which there is a negative pressure that allows the lungs to expand during inspiration. The right lung consists of three lobes (superior, middle and inferior) and the left has two lobes (superior and inferior). The base of each lung rests on the diaphragm, while the apex of each lung extends superiorly to a point about 2.5 cm above the clavicle [2]. The quantity of air that can be contained in the lungs is expressed as lung capacity (LC) and it changes according to the phase of respiration (3400-3700 cm^3 in an ordinary inspiration, 5000-6000 cm^3 in a forced inspiration). The respiratory air, i.e., the amount of air that is normally inhaled and exhaled, is about 500 cm^3. The volume of air that remains in the lungs between two breaths is called functional residual capacity (FRC). External respiration is divided into four main processes:

- pulmonary ventilation: the air moves in and out of the lungs, as volume movement;
- exchange of gases (oxygen and carbon dioxide), through diffusion, between the blood and the pulmonary air cavities;
- Transport of O_2 and CO_2 by the blood between lungs and tissues;
- Exchanges of the previous gases between the blood and the tissues.

Air flow, like blood flow, is a volume flow driven by a pressure gradient, present between alveoli and external air (atmospheric). Air movement depends on this gradient between areas of high pressure and areas of low pressure. When the pressure

in the alveoli is lower than atmospheric pressure inspiration occurs, resulting in a pressure gradient that introduces air into them, and vice versa for expiration. The pressure gradients are determined by the respiration muscles that modify the lungs volume. The relation between the pressure and the volume of a gas follows the Boyle law:

$$PV = nRT \tag{3.1}$$

where n is the number of grams moles of gas, P is pressure, V is the volume, R is the gas constant, and T is the absolute temperature. The air flow through the lungs is defined as volume flow and its speed is determined by a pressure gradient and a resistance according to the formula:

$$F = \frac{P_{atm} - P_{alv}}{R} \tag{3.2}$$

where F is the air flow inside the lungs, P_{atm} is the atmospheric pressure that at sea level is usually 760 mmHg, P_{alv} is the intra-alveolar pressure that at rest is equal to the atmospheric pressure (thus the differential is 0 mmHg), and R is the resistance to flow. The inspiratory process begins with nervous stimulation of the inspiratory

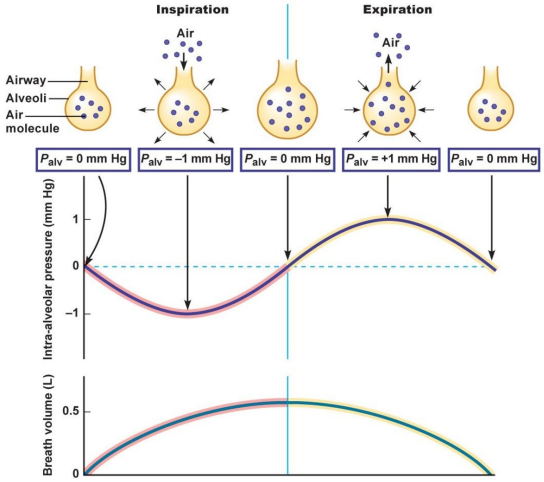

Figure 3.2: *The figure shows changes of the intra-alveolar pressure and of the respiratory volume during inspiration and expiration [5]*

muscles which causes the toracia wall to expand and increase its volume. This expansion exerts a pull on the intrapleural fluid, causing a decrease in intrapleural pressure which results in an increase in transpulmonary pressure [5]. As the lungs expand, the pressure in the alveoli drops below the level of atmospheric pressure, so air flows into the alveoli and continues to flow until the pressure reaches the level of atmospheric pressure again. Exhalation, on the other hand, is normally a

passive process, not requiring muscle contraction, but only the release of inspiratory muscles. The measure of the facility of the lungs to expand is called pulmonary compliance (PC), and it is defined as follow:

$$PC = \frac{\Delta V}{\Delta(P_{alv} - P_{ip})} \tag{3.3}$$

Where ΔV is the pulmonary volume change, e $\Delta(P_{alv} - P_{ip})$ is a transpulmonary pressure change. The movement of oxygen and carbon dioxide between the alveolar air and the blood is obtained by diffusion and depends on the concentration gradient. In the alveoli oxygen is in a major concentration and for this reason diffuses into the blood, while carbon dioxide follows the reverse direction. Oxygen is transported in the blood by haemoglobin, a protein with a special structure that allows oxygen to be bound and released at the right time. Haemoglobin consists of four subunits, each of which contains a globin (globular polypeptide chain) and a heme- group, which contains iron [stanfield]. The bond and release of oxygen is regulated by the P_{O_2} of the environment that surrounds the haemoglobin. High P_{O_2} favour the bond of the oxygen with the haemoglobin, while a low P_{O_2} facilitates the release.

Chapter 4

Ultrasounds

Ultrasound to date is the most widely used imaging technique, and the number of ultrasound devices in the region is almost 10 times that of any other device. These are the principal reasons for this diffusion:

- It is the first device that uses non-ionizing radiations because it produces mechanic waves that are unable to ionize matter and if used well do not create significant negative biological effects;
- Ultrasound devices have the highest temporal resolution with devices that arrive at 300 images/s. These devices can monitor evolving state without problems, and they show real-time images;
- Ultrasonography is a user-friendly technique because it is a non-invasive, simple, low-cost, and rapidly performed method.

However, this technique also has some disadvantages and limitations:

- it is "operator-dependent" so the accuracy of acquisitions and analysis is highly dependent on the experience and skills of the clinician;
- scatter limits the maximum depth of sound penetration;
- the absorption of the US is frequency-dependent
- it cannot be used to scan structures and tissues that have bone or gas on them because these elements have very high and very low acoustic impedance,respectively

4.1 Physics and generalities of ultrasound

Ultrasounds are mechanical waves, longitudinal elastic waves of rarefaction and compression, with a frequency higher than the upper band limit of the human

audible, thus higher than 20 kHz. These waves propagate within tissues transferring only mechanical energy to them; there are no electrical or magnetic components and they are easy to focus and concentrate in very small sources. They are described by wave mechanics notations: frequency, intensity, wavelength, amplitude, and propagation speed. Frequency is the inverse of period and it is number of times the wave repeats per second, and is expressed in hertz. In diagnostic the frequencies fall between 1 and 20 MHz and the frequency utilized influences the penetrating ability. Intensity is the energy flowing in unit time through a uniform surface perpendicular to the wave propagation and is proportional to the squares of the amplitude and pulsation of the wave, and it is generally expressed in decibels. The wavelength is the distance between each compression or rarefaction band, consequently is the distance travelled during a cycle or period. Amplitude represents the maximum variation of the wave. The propagation speed depends highly on the medium of transmission and ultrasounds are not able to transmit in a vacuum because there are no molecules present. The link between the ultrasound speed in a medium and the frequency of the ultrasound itself is expressed by the following relationship:

$$v = \lambda f \tag{4.1}$$

Where v is the propagation speed, f is the wave frequency and lambda is the wavelength. The wavelength turns out to be a measure of the minimum spatial resolution one must have within an image. The higher the frequency, the better the quality of the image we obtain. In particular, the following eqution shows how to obtain the velocity of US in human liquids and tissues:

$$\sqrt{\frac{E}{\rho}} \tag{4.2}$$

where ρ is the density of the material, expressed in kilograms per cubic meter and E is the Young's modulus. For most tissues the velocity varies between 1500-1600 m/s, but the most common value for biological tissues is 1540 m/s, so many instruments are calibrated to it. In some devices optimized for abdominal scanning, a speed of 1550 m/s is used because it is the propagation speed of the liver, the most important and studied organ in the abdomen. In practice, however, no major differences are observed between scans obtained at 1540 m/s and 1550 m/s. Another important characteristic is the acoustic impedance (Z) that is also related to the speed of US propagation. It is defined as the product between the density of the medium and the speed of propagation in the medium itself.

$$Z = \rho v \tag{4.3}$$

Acoustic impedance is a fundamental characteristic since it is precisely it that generates the reflection and scattering phenomena of the US. In the following table are shown the impedance values of the main tissues of the human body.

Material	**Density** (kg/m^3)	**Propagation speed (m/s)**	**Acoustic impedance** ($kg/m^2/s * 10^6$)
Air	1.2	330	0.0004
Water	1000	1480	1.48
Media soft tissue	1060	1540	1.63
Liver	1060	1550	1.64
Muscle	1080	1580	1.70
Fat	952	1459	1.38
Brain	994	1560	1.55
Kidney	1038	1560	1.62
Lung	400	650	0.26
Bone	1912	4080	7.80

Table 4.1: *Density and acoustic impedance of air, water and biological tissues with propagation rate of US in them.*

4.1.1 Us generation and beam geometry

Special materials called piezoelectrics are used to generate ultrasound. these are materials, in the form of crystals, that can transform an electrical quantity into a mechanical quantity and vice versa. the phenomenon of piezoelectricity is divided into two main effects:

- direct piezoelectric effect: a ΔI change in the size of the crystal causes a change in ΔV potential between the faces of the crystal;
- inverse piezoelectric effect: a ΔV change between the potential of the crystal faces causes a compression or ΔI expansion of the crystal itself.

In ultrasound devices, therefore, their generation is achieved by piezoelectric crystals by exploiting the inverse piezoelectric effect. The crystals are properly voltage driven and generate a vibration transferred to the patient's tissues by contact. In addition, using the direct piezoelectric effect we can also measure the ultrasounds reflected by the tissues. The mechanic wave reflected hits the sensors, causes their mechanic deformation that becomes a variation of electric potential.

Initially quartzes were used as crystals, today a ceramic filled with different elements (phosphorus, zirconium, and titanium) with the following abbreviation is used: PZT. They emphasize the piezoelectric effect and have a longer mechanical durability, but they are fragile, so they need to be treated with care. Geometric dimensions of the crystal are very important because they are related to the frequency generated:

$$f = \frac{2}{h} \tag{4.4}$$

Where h is the thickness of the plate. Therefore, the smaller the crystal the higher the resonance frequency. In the beam emitted by a single transducer, a proximal zone and a distal zone are identified, in the latter the beam diverges. The extent of the proximal zone is given by:

$$L = \frac{d^2}{4\lambda} \tag{4.5}$$

Where d is the dimension of the crystal, L is the length of the proximal zone and lambda is the wavelength. The beam, in order to be used on ultrasound devices,

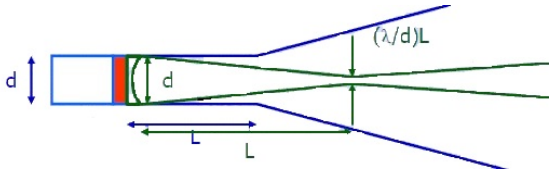

Figure 4.1: *The figure shows the geometry of a US beam and demonstrate the necessity of the focusing process.*

will be subjected to the focusing process. The zone of maximum focusing is called 'focal area' while the point of maximum collimation is called 'focus'. The beam can be focused through two different techniques: mechanical focusing and dynamic focusing.

Spatial resolution

The effective resolution of a US device depends on how the ultrasounds are emitted. Spatial resolution theoretically coincides with the wavelength, but in practice this is not true. A pulse made by several sine cycles exits from a probe. This packet propagates into the tissues; upon encountering a first discontinuity it will be partially reflected and return back to the probe. At a second discontinuity it will be reflected again creating a second packet back to the probe. If the length of this initial packet is less than the distance d between the two interfaces the packet generated by the first reflection and any packet generated by a second reflection

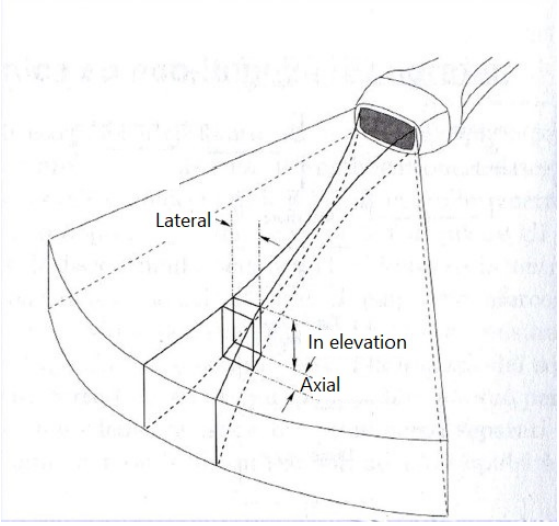

Figure 4.2: *The figure shows the field of a real probe and its three resolution directions: axial, lateral and in elevation.*

return to the probe at different times. But if this distance is less than the distance d the two return echoes arrive at the probe overlapping. So, it is the duration of the packet that defines the actual spatial resolution of the device. However, we cannot emit packets that are too short since we would have a return echo with a bandwidth too wide. The compromise is to emit a packet that has a sine wave cycle content ranging from 3 to 5 with some exception. The field of a real probe is placed in a three-dimensional fan. Therefore, there are three resolution directions: axial, lateral and in elevation. For modern probes, however, it is important to have a good axial resolution, that is, the ability to distinguish two objects on the path of the ultrasound moving away from the probe.

4.1.2 Propagation and reflection of a US wave

As we mentioned earlier, acoustic impedance is a very important characteristic because it generates the reflection and scattering phenomena of the US. The amplitude of the return echo is proportional to the difference in acoustic impedance between two tissues. The principle of reflection is the same as we can observe in geometric optics. Considering the image 4.3 we have R that represents the reflected wave, I that represents the incident wave, and T that represents the transmitted wave. Supposing we have a surface characterized by two materials with two different refraction indexes n_1 and n_2, the radiation hitting the surface is partly reflected and partly transmitted. The angle of reflection θ_1 is equal to the angle of incidence while the angle of refraction is different, and its sine depends on the ratio between

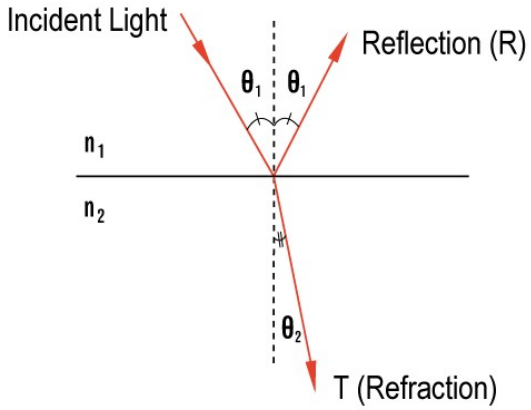

Figure 4.3: *The figure shows two material with different refraction indexes, T represents the transmitted wave, I the incident wave and R the reflected one. The ratio of the sines of the angles of incidence θ_1 and refraction θ_1 is equivalent to the ratio of the velocities in the two media.*

n_1 and n_2 as follow:

$$\frac{sin(\theta_1)}{sin(\theta_2)} = \frac{v_2}{v_1} = \frac{n_1}{n_2} \tag{4.6}$$

This is called Snell's Law and n_1 is the refraction index in the first medium and n_2 is the refraction index of the second medium, θ_1 is the incidence angle, θ_2 is the transmitted angle, v_1 is the velocity in the first medium, v_2 is the velocity in the second medium. Given the impedances of the two materials, it is possible to calculate the reflection coefficient (R) with the following equation:

$$R = (\frac{Z_1 - Z_2}{Z_1 + Z_2})^2 \tag{4.7}$$

The sum of the transmission coefficient and the reflection coefficient (T) must be equal to one. Hence we have the following relation:

$$T = 1 - R \tag{4.8}$$

An ultrasound image is nothing more than a spatial representation of all the points at which the ultrasound has encountered a discontinuity which will have generated a return echo. The ultrasound beam is transmitted through the body in the form of acoustic energy, described as intensity or power. Tissues attenuate in terms of acoustic impedance the ultrasound that was able to propagate. If we have an ultrasound beam of initial amplitude A_0 propagating along a scan line in the z-direction and we want to see how from the initial amplitude the ultrasound

Tissue	Absorption (dB/MHz cm)
Air	-
Fat	0.5
Muscle	2
Liver	0.7
Brain	1
Compact bone	4-10
Water at 20°C	0.002

Table 4.2: *Rate of absorption of tissues*

amplitude decreases as it propagates through the tissue, we find that the amplitude decreases as an exponential, as follow:

$$A(z) = A_0 e^{-\alpha z} \tag{4.9}$$

The constant, alfa, that determines how fast decreases acoustic impedance is specific for each tissue.

4.2 US devices: equipment tools

The principal components of an ultrasound device are shown in the figure 4.4 and they are: the pulse generator that stimulates and drives the piezoelectric crystals, the probe, which can have a dual role of emitting and receiving echoes, the receiving circuit consisting of an acoustic demodulator, which goes to search for a pulse of known frequency within the noise, an amplifier time gain compensation (TGC), which compensates the amplitude of the received signal with a gain proportional to the time elapsed between pulse emission and the reception of the return echo, a scan converter and a monitor to visualize the images.

4.2.1 Pulse generator

The pulse generator is always present, and it is a radiofrequency generator which is responsible for generating the electric field at the desired frequency (in this case ultrasound frequency). Synchronized high-voltage pulses are sent to the piezoelectric crystals in the probe. The pulse length determines the axial resolution and usually varies between 0.1-1.1 mm, and there must be enough time between two pulses to allow the return echo to reach the transducer before the new one. The repetition rate of the pulses can be adjusted. There are two types of emission

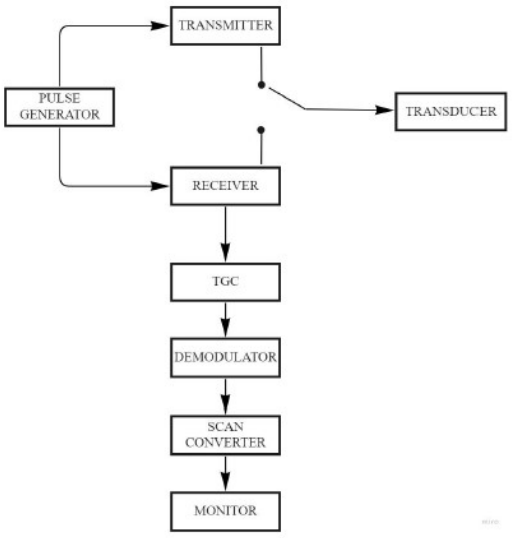

Figure 4.4: *Block diagram of an ultrasound device. The main components are shown.*

modes: pulsed and continuous. In the second case, the crystals are divided between those that emit and those that receive.

4.2.2 Probe

The ultrasound probe is the instrument that transforms electrical energy into mechanical energy, in the form precisely of ultrasound waves, and vice versa. Because of this characteristic it is called a duplex transducer. The most important part are the piezoelectric crystals whose properties, described above, allow precisely the phenomenon of energy transformation. They, inside the probe, are protected and isolated acoustically and electrically by encapsulation in a matrix of epoxy resin or other similar material. Modern probes consist of array of sensors that can have different geometric arrangements. There are four different types of probes:

- Linear array probes: crystals are arranged along a line. These probes have the highest number of crystals, from a minimum of 128 to a maximum of 256. Linear probes are suitable for surface applications and thus for the investigation of what is 3 to 4 cm below the skin, but with a very high resolution. They are high frequency probes with a typical range of 5 up to 15 MHz. They have the disadvantage of requiring a large contact area with the skin, so they are not suitable for sub-sternal or intercostal ultrasound.

- Convex array probes: crystals are arranged along a curve. Typically, the ray

of curvature is 60 mm and they have a number of crystals which goes from 100 to 120. The frequency range is smaller, from 2 to 7 MHz, because the emission frequency of the probe is lowered to reduce the attenuation imposed by the tissues. The acoustic field fans out in depth, basically it widens as it propagates, and it is therefore possible to observe a relevant portion of organs and tissues at the same time. The investigation depth is of 15-20 cm and for these reasons this is the election probe for abdominal organ scans, thoracic and abdominal tract vascular type scans, and obstetrics and gynaecology scans.

- Phased array probes: they can steer the beam as desired by appropriately driving the crystals. The probe has a small support base but can generate a beam in every direction. It has three main applications, that is, the transthoracic echography, the transcranial echography and the paediatric field.

- Microconvex probes: they are invasive probes, have a shape that fits the investigation done from the inside and are called cavitary probes. Every cavitary probe is a convex probe, that is, the emitted field is always divergent in a larger or smaller fan-shaped pattern depending on the organ to be investigated. The frequency can be raised, 4-10 MHz, because we have less tissue to go through.

4.2.3 TGC

When the US propagate and are reflected due to acoustic impedance discontinuity two things happen:

- Reflexion effect: the US pulse finds an area where there is a discontinuity of acoustic impedance, and according to the reflection coefficient some of the energy goes back to the source;

- Tissues attenuation: the US pulse loses intensity with propagation, when it finds a discontinuity, it is reflected and on the return journey it again undergoes attenuation. So, when it reaches the probe, the echo amplitude is not only a function of the reflection coefficient value but also of the attenuation.

The TGC is specifically used to compensate for the depth effect that is superimposed on the effect of the reflection coefficient when an echo arrives at the probe. Its task is then to rebalance the amplitude of the echoes so that it returns to being dependent only on the reflection coefficient. If we want to compensate for the effect of attenuation, that is a decreasing exponential, the amplifier must have a logarithmic law, so the TGC is a logarithmic amplifier that takes time-of-flight as input. In this way shallow echoes are amplified very little and as the echo is deeper and deeper it is amplified more.

4.2.4 Demodulator and scan converter

These two blocks basically serve to convert the amplitudes of the received echoes into numerical values and to fill a video matrix that will be the image shown on the monitor. In particular, the demodulator governs the dynamic by which a numerical value is assigned to a given echo amplitude.

4.3 Display modes

With the ultrasound scanner, ultrasound data can be displayed in different modes. There are four main strategies used:

- A-Mode: it is the Amplitude mode, and it is no longer used in common devices. The probe investigates a single scan line and every time there is a discontinuity of acoustic impedance an echo returns to the probe and on the monitor is shown the amplitude of the echo that has arrived from the area as a function of depth.

- B-Mode: it is the Brightness mode, and it Is the principal mode utilized. Each pixel in the image has a brightness that is proportional to the amplitude of the echo returned [2]. This mode is usually used to examine organs and foetus status.

- M-Mode: it is the Motion mode. This mode is only used in cardiology and its function is to see how certain points move over time in the tissue and to quantify this movement. The probe has a single scan line along which the beam encounters acoustic impedance discontinuities that can be mobile. Signals reflected structures are converted into waves that are shown continuously along the vertical axis [2]. Often used with B-Mode in duplex modality.

4.4 US devices for flowmetry

These devices are used to measure the emetic flux characteristics and velocity. The basic principle utilized to measure this quantity is the Doppler effect. The Doppler effect is the change of the frequency of sound when the sound waves are reflected from moving targets, in this case red blood cells. The receiver senses a different frequency depending on the motion of the source: higher frequency if we have an approaching motion (positive shift) and lower frequency if we have a receding motion (negative shift). The difference between the transmitted and received frequency is called the Doppler frequency, or Doppler shift, and is proportional to the velocity of the target. The definition of the Doppler frequency (f_d) is given

below:

$$f_d = \frac{2f_0 v}{c} cos(\theta) \tag{4.10}$$

Where f_0 is the initial frequency of the US wave, v is the velocity of the erythrocytes, θ is the angle formed between the probe scan line and the direction of propagation of the erythrocytes and c is the velocity of US propagation in the tissue (1540 m/s). If the probe emits at a frequency equal to f_0 what goes back to the probe after hitting a vessel is $(f_0 + f_d)$ if the flow is approaching and $(f_0 - f_d)$ if the flow is receding. From the equation above we can make some observations:

- Doppler flowmetry cannot be performed by insonating a vessel orthogonally since $cos(\theta) = 0$ and there would be no more doppler rejection. Normally for anatomic districts it is maintained an angle between 40° and 60°.
- the deviation in frequency is proportional to the frequency of the emitted US f_0
- the deviation is a function of the angle
- If the blood velocity is between 0 and 1 m/s and if f_0 is in the range 1-10 MHz, Δf is 0-12 kHz, i.e., it is within the audible band and can be directly heard.

The velocity is calculated as follow:

$$v = \frac{c}{2f_0 cos(\theta)} f_d \tag{4.11}$$

Echo doppler is also used to assess:

- The vasculature of tumours and organs.
- Cardiac function.
- Occlusion and stenosis of blood vessels.
- Blood clots in blood vessels.

Two types of flowmeters exist: continuous wave flowmeters and pulsed wave flowmeters. In the firsts the probe emits continuously the acoustic wave, and they are used to measure status in which velocity is very high due to pathological conditions. In the seconds a wave is emitted and then the echo is expected and they permit to measure the blood velocity profile in a specific point of the vessel.

4.5 Artifacts in ultrasound images

Artifacts arise because assumptions are made about the physics of the US that are not always met, thus going to create a sliding between reality and the physical modelling exploited. We can group the artifacts into four macro groups based on the assumptions made:

- US generation: narrow and uniform US beam in amplitude
- Geometry of the US beam: straight path of the US beam
- Constant velocity independent from the crossed tissue
- Uniform tissues attenuation.

Typical artifacts effects that we can observe are:

- Not real images;
- Lower density and/or luminosity;
- Higher density and/or luminosity;
- Echo absence and images lost;
- Echo reinforcement;
- Shadows;
- Structures dislocations;
- Wrong shapes and/or dimensions.

4.5.1 Tissues attenuation

In this group we can find two type of artifacts:

- Shadowing: it arises from the presence of very absorbent tissue. The US signal arrives behind this material with lower energy and for this reason a shadow cone, called acoustic shadow, is created. The tissues that generate this artifact are collagen-rich tissues, kidney stones, calcification and plaques.
- Enhancement: it is the contrary of the shadowing. The intensity of the downstream echoes of a liquid collection increase and the tissues behind this collection emit very high signals which are therefore reinforced with respect to the surrounding tissues

4.5.2 US generation

This assumption stats that we have a narrow and uniform US beam in amplitude and that each structure generates a single reflection. In this macro group we can find these artifacts:

- Boundary shadows: it is caused by the reflection and refraction of the US beam.
- Reverberation: it occurs at a wide and highly reflective areas. Part of the US wave is reflected and starts to oscillate between the hyper-reflective walls of two structures. The echoes received from the transductor at different times and with different intensities, due to multiple reflections, give a false information about the existence and deepness of the tissue. This artifact is more evident with the growing intensity of the reflected signal.
- Comet tail: it is a particular artifact of reverberation between the transductor and the reflective object and between the front and rear interface of an object (inner reverberation). Small dimensions reflective structures present very close reverberations which create a comet tail effect, that is many small parallel bands of echoes arranged transversely to the direction of the US beam. They are tighter as we get away from the element that generated them which is why the comet tail often has a triangular shape with a vertex downstream. This type of artifact is generated from the presence of gas in cavities, vessels and ducts, from calcifications of various nature, from metal catheters, plastic material and probes elements and from clips or foreign bodies.

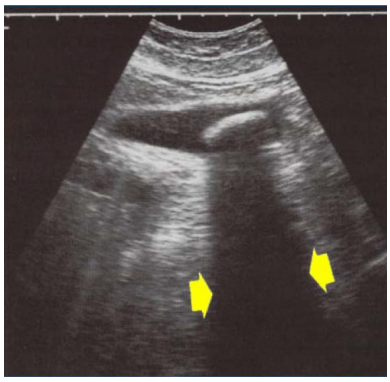

Figure 4.5: *The figure shows an example of the shadowing artifact*

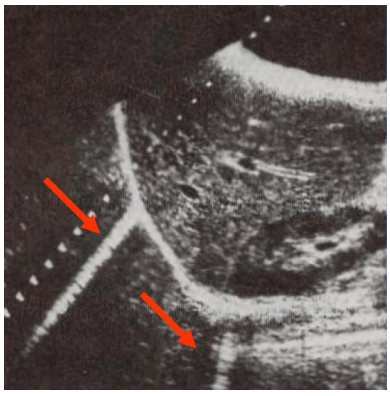

Figure 4.6: *In this figure, instead, is shown an example of the comet tail artifact*

- Mirror: a formation, placed between the transducer and a very reflective interface, determines a second reflected image. This second image will be placed downstream with respect to the interface and along the direction of the US beam. We can have an axial reflection, in which the reflective interface is nearly perpendicular to the US beam, and a non-axial reflection, in which the interface is a little curved and so it is not generated just below the US beam.

4.5.3 Geometry of the US beam

Almost all transducers used in medical applications are focalised, so the beam is not straight and uniform but has an hourglass shape. The applied simplification therefore generates the following artifacts:

- Lateral lobes: the US beam it is not perfectly bounded; in its lateral portions there are components of lesser intensity. While the central portion of the bundle reaches the internal part of the formation (e.g. liquid cyst) the lateral lobes of the bundle interact on the latero-lateral walls of the same. It follows the representation of echoes, detected by the device, within the image of the formation itself.
- Axial and/or lateral resolution: the resolution is the ability to clearly distinguish the edges of two adjacent points and it can determine the loss of detail. The axial resolution is determined by the length of the pulsation time, while the lateral resolution is determined by the width of the US beam.
- Beam width: it is observable when there are structures in the beam distal zone that generate detectable echoes. This artifact could be reduced by modifying the focal zone or the focal point.

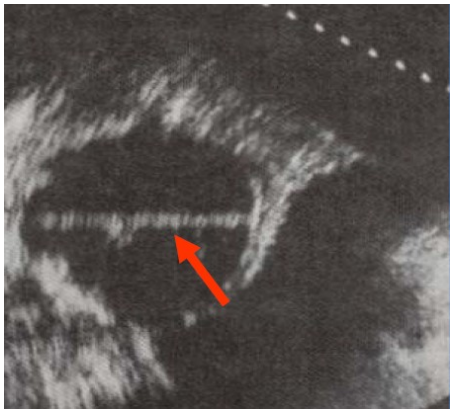

Figure 4.7: *The artifact due to lateral resolution is shown in the figure above*

4.5.4 Sound velocity

These artifacts born because the sound velocity is not always constant into the different tissues. the main artifact that can generate from this problem is the geometric distortion. If the propagation velocity into the tissue is less than 1540 m/s, the distance calculated between the probe and the tissue is smaller and so the structure will be represented more deeply. On the contrary, if the propagation velocity into the tissue is higher than 1540 m/s, the distance calculated between the probe and the tissue is bigger and so the structure will be represented more closely. In the end, when there is a velocity variation with a refraction of the US, a profile break in the tissue can be seen.

Chapter 5

Hydration and body fluid balance

Water is the most important defining element of life, and it is essential in our organism. Suffice it to mention that water contributes 50-70% of total body mass and is compartmentalized within intracellular (65%) and extracellular (35%) [7]. Water is essential for its ability to keep in solution the precursors and products of our metabolism, and to allow their transport in the body [8]. Water is also essential to:

- Maintain blood volume.
- Transport nutrients.
- Remove metabolic waste through hepatic and renal way.

For these reasons, a good level of hydration is fundamental to keep the Total Body Water (TBW) content within the right levels and to maintain an optimal state of well-being. It is estimated that to achieve this objective it is necessary to introduce 2-3 L of liquids per day, equal to the amount eliminated daily by the body, mainly for thermoregulation and with urine [8]. If the intake of fluids is not enough or if we are submitted to a prolonged exercise that cause the loss of hypotonic fluid in the form of sweat, the organism can enter a condition of dehydration. Dehydration is typically defined as acute weight loss of 1% to 2% of body weight [9] and it increases cardiovascular strain. In particular, the loss of the 2% of body weight is dangerous for the organism and can provoke different disorders such as cardiovascular strain, hyperthermia, physical performance and concentration reduction, heat cramps and, eventually, death. That is why fluid balance is crucial for the athlete's optimal performance and safety during exercises [7]. Sweating, that increases the dissipation of heat to the environment through

Average Intake per Day	Average Output per Day
Metabolism, 10%, 250ml	100ml, Faeces, 4%
Foods, 30%, 750ml	200ml, Sweat, 8%
Beverages, 60%, 1500ml	700ml, Insensible loses: skin and lungs, 28%
Total Intake, 2500ml	1500ml, Urine, 60%
	2500ml, Total output

Table 5.1: *Balance of human fluid. [7]*

evaporative cooling, can be of only 100 mL/hour during a moderate activity but can go up to 3 L/hour for a prolonged or vigorous exercise in a hot environment. This results in a decrease in total body water volume. Many factors influence the hydration status of the human body:

- Availability of fluids
- Environmental conditions
- Structure of exercise
- Intrinsic factors and sport-specific factors

In the athletic setting, hydration status is most often assessed by monitoring weight and urine concentration [9] at the first urination of the morning. When more precision of acute hydration changes is desired, plasma osmolality, isotope dilution, and body mass changes, used in appropriate context, provide for the accurate gradations in measurement often required in research [10]. For urine concentration the markers used to estimate dehydration are a reduced urine volume, a high urine specific gravity (USG), a high urine osmolality (Uosm), and a dark urine colour (Ucol). For the body mass, instead, acute changes in hydration are calculated as the difference between pre- and post-exercise of it (this technique implies that 1 g of lost mass is equivalent to 1 ml of lost water). The level of dehydration is best expressed as a percentage of starting body mass rather than as a percentage of TBW because the latter varies widely [10]. These two methods are simple and non-invasive but also not immediate and rapid. It was therefore thought to exploit the sonographic measurements, a quick and easy method, of the inferior vena cava (IVC). In fact, ultrasound determination of the IVC diameter is a valid marker of volume status and, therefore, hydration in the individual. The venous district can

provide useful indications for the assessment of hydration status through the ability of veins to collapse during respiratory dynamics. Static and dynamic observation of the IVC, the supra-hepatic veins and the jugular veins, provides useful indicators for the estimation of hydration by means of the vessel caval index (CI) obtained from the ratio of the difference between the vessel diameters in the expiratory and inspiratory phases to that of the expiratory phase. In particular, the first two are observable by means of a convex probe (used in this study). Normal values of the caval index are between 0,75 and 0,40: CI values above 0,75 express dehydration, while values below 0,4 indicate hyperhydration [11].

Chapter 6

Materials and Methods

6.1 MicrUs EXT-1H

The firm Telemed deviced an open architecture diagnostic system based on ultrasound called MicrUs EXT-1H. It is a very flexible and versatile technology because it exploits the USB power supply, the fan less technology and can be used on PCs, tablets and smartphones. It allows the use of a wide range of multi-frequency transducers with wide bandwidth, from 2,0 to 15,0 MHz, which enables high image quality in various clinical fields: general, abdominal, obstetrical-gynaecological, small parts, musculo-skeletal, urological, ultrasound-guided procedures, etc. The supported probes are linear, convex, micro convex, and endo-cavitary with a deepness that goes from 2 up to 31 cm depending on the probe used and the display modes are various (including B and M mode). To use the architecture, the company provides the beam-former and wiring (USB); the user must download the software and drivers contained in the USB drive, also provided at the time of purchase. To start the acquisition procedure you will need to connect the beam-former to the PC (via USB wire) and then connect the probe to the beam-former. Thus you are ready to start an ultrasound acquisition, the display of which will be calibrated according to the resolution of the laptop monitor.

6.2 ECHO WAVE II scanning software

The system is driven by the ECHO WAVE II scanning software with an intuitive user interface shown in the figure 6.1. On the left side of the panel are several parameters that the user can change to adjust image quality and improve performance. The most important controls to adjust are: scan depth, gain, TGC and focus. First of all, the depth changes depending on the type of body region to be scanned, specifically a larger, inner area requires a greater depth value and vice versa.

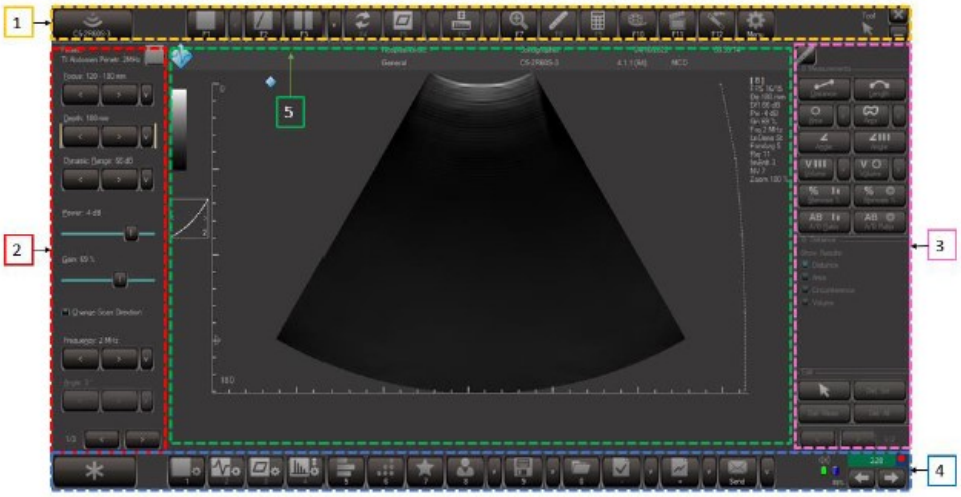

Figure 6.1: *The figure shows the user interface of our scanning software.*

Greater depth can also be obtained by selecting a low value for the ultrasound probe frequency. Secondly, gain and time gain compensation (TGC) play a key role in the reception of the signal to the probe, namely the return echo. The body tissues in fact attenuate the mechanical wave, and it is therefore essential to use the TGC parameter to compensate for the depth effect that is superimposed on the effect of the reflection coefficient when an echo arrives at the probe. Moreover the gain parameter has an effect over all return signals, it in fact act on brightness of the image acquired, which is the sum of signals coming from different depths. Finally, the focus parameter turns out to be useful for varying the resolution in specific areas through the use of special markers. Specifically, the software allows you to choose the depth and area of focus. After the proper captures are completed, several operations can be performed including a saving of the videos or images either in .mp4 or .avi format or other similar formats. However, it is possible to work and perform measurements both on newly collected images and on images previously saved in memory. The software eventually allows to archive this data and create an actual report for each subject analyzed. At least there are some parameters that the user can set. Firstly, the Dynamic Range it works on contrast, that is, the parameter changes the gray scale by increasing or decreasing gray tones. By doing so, it is possible to more accurately detail structures with different acoustic impedance that otherwise would not be distinguished from one another. The Color map values might be set through the Palette, and it works on brightness and darkness of each image level. The quality of an image is based also on the noise reduction, therefore to limit it can be used two commands: Frame averaging

and Rejection. Overall there are several default configuration (Presets) which can be selected depending on the probe used and the examination to be performed. The user is able to add presets if he deems it necessary.

6.3 Ultrasound probe

For this study, a Convex-type probe, C5-2R60S-3, manufactured by the company Telemed, was used (figure 6.2). The crystals on the probe are S3 type and the transducer can work in the frequency range of 2-5 MHz. It has a bending radius of 65 mm and a field of view of 60°. The main applications are for abdomen, gynecology, and pediatric ultrasound. [12]

Figure 6.2: *The figure shows the Convex probe C5-2R60S-3.*

6.4 Treadmill Reharunner 02

A treadmill model Reharunner 02, from Chinesport S.p.A., Italy, was used to exercise the candidates and thus induce sweating. The system is CE-marked, and

Figure 6.3: *The figure shows the treadmill Reharunner 02*

Figure 6.4: *The figure shows the detail of the treadmill display and settings. In particular we can set the velocity and inclination and during the exercises the cardiac frequency and its trend is directly shown on the display*

the walking parameters can be set from the on-board computer, which allows adjustment of the belt speed and incline. Further settings can be customised from the control panel. It has a walking surface of 154 x 54 cm and supports a maximum working load of 180 kg. The device is mains-powered (220-240 V, 15 A, 50-60 Hz) and draws a maximum power of 2000 VA. The maximum permitted speed is 25 km/h, and the maximum inclination is +30%.

6.5 Impedance scale

The scale used is a Tanita brand commercial scale, model BC-730. It uses bioimpedance analysis to measure body composition by sending a safe, low-frequency signal throughout the body from the 4 electrodes placed in the base of the scale. This signal circulates through muscle tissue fluid, stopping when it finds resistance from fat tissue. This resistance, called, Bioimpedance, is calculated accurately and its results change depending on a person's gender, height and weight to give a personalised fat and body composition reading. It is possible to use it in 'guest' mode, allowing the age, gender and height of the person to be weighed to be selected. The parameters returned are total body weight, body fat percentage, visceral fat index, muscle mass, physical index, bone mass, BMR, metabolic age and total body water. the device is powered by batteries and has 4 impedances on which the subject's feet are placed. To ensure accuracy, the manual recommends taking measurements

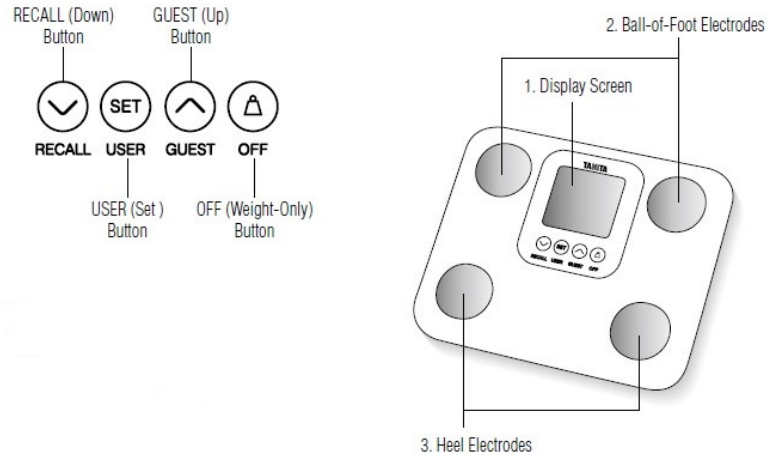

Figure 6.5: *The figure shows the Tanita BC-730 scale and its settings.*

undressed and if this is not possible to always remove the socks anyway. In our case, as it was not possible to have the candidates completely undressed, the second recommendation was followed, so the candidates were weighed barefoot. Heels must be correctly aligned with the electrodes on the measuring platform and even

if the feet appear too large for the unit, accurate readings can still be obtained if the toes overhang the platform [13]. The scale has a compact design (21.6 x 26 x 3.5 cm) and the maximum user weight supported is 150 kg with an accuracy of 100 g on total body weight and 0.1 % on body fat.

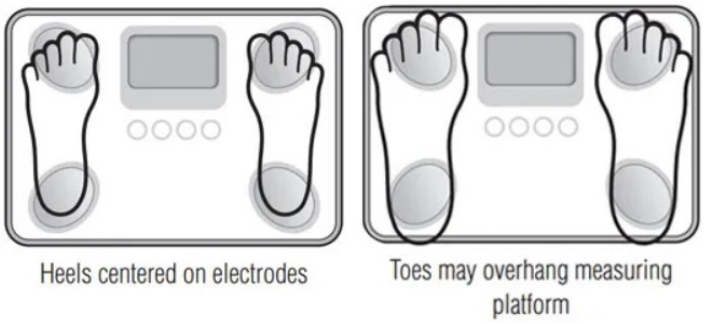

Figure 6.6: *The figure shows the right placement of the feet on the four impedances placed on the surface of the scale.*

6.6 Heart rate sensor Polar H10

During the exercise to monitoring the heart rate and the frequency of the candidates a Polar H10 heart rate sensor has been used. It is a very precise heart rate sensor that comes with the Polar Pro chest strap, and provides interference-free electrical measurement. Polar H10 connects and transfers data via Bluetooth® and ANT+™

Figure 6.7: *The figure shows the polar H10 complete with belt and sensor*

Figure 6.8: *The figure shows the electrodes area on the polar H10 belt provided with the sensor*

and so it has a variety of connection possibilities with compatible sports watches, smart watches and training apps [14]. In our study we used the ECG logger app that permits to register the entire ECG tracing in a .csv format. The plastic electrodes areas on the reverse side of the strap detect heart rate and the connector sends this heart rate signal to the receiving device (in our case a smartphone). The Polar H10 has a CR 2025 battery with a lifetime of nearly 400 h. It can operate in

the following range of temperatures: -10 °C to +50 °C. For optimal detection, the belt should be positioned just below the chest and to ensure sufficient transmission range from the Polar H10 heart rate sensor to the receiving device, the device should be kept in the front.

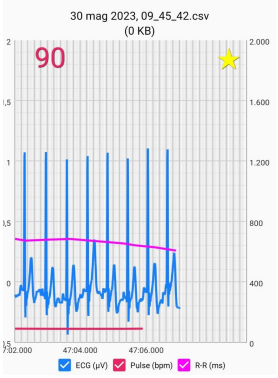

Figure 6.9: *The image shows an example of an ECG waveform measured by the H10 polar band and viewed and logged via the ECG Logger smartphone app. In particular this is the app layout*

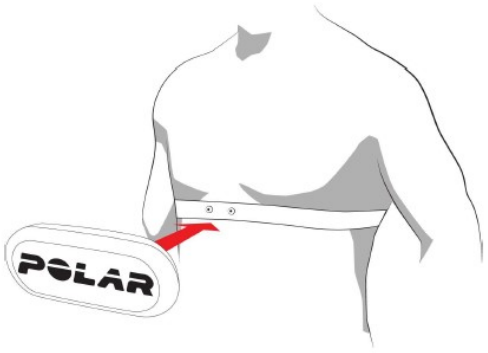

Figure 6.10: *The figure shows the correct way tho wear the belt, with the electrodes, and the heart rate sensor to ensure a correct detection and transmission*

6.7 Tests conducted

To evaluate the variation of diameter of the inferior vena cava after a loss of hydration, we subjected some candidates, amateur/semi-professional athletes, to a physical test to induce consistent sweating in them. First of all, some measurements were taken to obtain a baseline to be compared with subsequent measurements taken during and after the test. In particular, the candidates were weighed with the impedance scale described above, to detect body weight and percentage of total body water, they underwent an initial vena cava scan with ultrasound (video of approximately 10-15 seconds) and finally they wore the Polar H10 band to detect ECG and resting heart rate. During the test they were asked to wear sports clothing consisting of shorts and a short-sleeved shirt. The candidates were then subjected to a sustained uphill walk on the treadmill, with a speed of 5 km/h and 10% incline as initial parameters, for 10 minutes followed by a 5-minute break during which new weight and IVC scan measurements were taken. This routine was repeated 4 times for a total of 40 minutes of exercise interspersed with the respective measurements. The speed and slope parameters were adjusted during

the tests according to the candidate's sweating rate. At the end of the last task, the candidates were asked to rehydrate with an appropriate amount of water based on the fluid lost (calculated from the weight loss measured by the scales). During rehydration, a new ultrasound was performed to monitor the filling of the vein and every two minutes thereafter to check the change in size of the inferior vena cava following fluid replenishment. 30 candidates were tested, 14 women and 16 men of whom 7 volleyball players, 3 soccer players, 5 people training in the weight room, 1 basketball player, 1 martial arts practitioner, 1 athletic practitioner and 1 swimmer. The other candidates did not play any sport. During the examination, candidates were lying on an ultrasound couch in a supine position [15]

6.7.1 Dataset Construction

First of all , starting from the candidates that underwent the testing protocol, a dataset was created. This dataset is shown in the graph below. It contains the

Figure 6.11: *Dataset of subjects with the following informations: Age (upper right), Gender (upper left), Weight (Lower right), Body water(lower left).*

information acquired from each subject such gender, age or weight, and provides an overview of the characteristics of its subjects, which will be useful when a statistical analysis is performed on the results obtained. From each subject of the dataset the following ultrasound videos have been acquired over time:

- At the starting point: baseline IVC;
- In the sweating phase: IVC after 10 minutes of activity, IVC after 20 minutes of activity, IVC after 30 minutes of activity, IVC after 40 minutes of activity;
- In the hydration phase: IVC immediately executed, IVC after 2 minutes, IVC after 4 minutes, IVC after 6 minutes, IVC after 10 minutes.

After collecting data from each step of activity, it was possible to run a series of graphs showing weight trends over time and see what the trend of the subjects was. The result is shown in the following graph: The above graphs are included

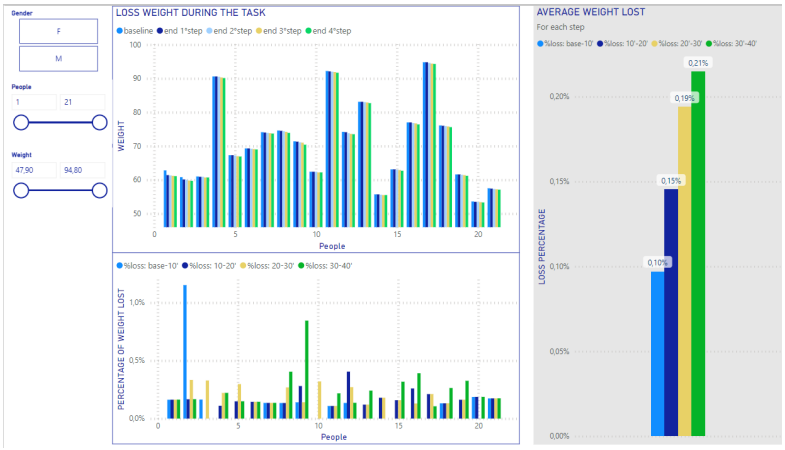

Figure 6.12: *Up Left:weight for each subject in each step, Low Left:% of weight lost; Right:average of weight lost for each step*

in an extensive report, created using the Microsoft Power BI tool, which provides an overview of all the stages of the project and all the steps taken to arrive at the measurement of the variables of interest such as diameter and caval index. The final report can be found at the following link :

6.8 IVC ultrasound

When an IVC echo is performed, the user investigate a treat of body of almost 20 centimeter, placing the probe on the right of the body mid-line, just under the rib cage to see the last part of right atrium and the initial treat of the IVC. The vein continue until the sub diaphragmatic zone. In addition, in order to execute an optimal ultrasound acquisition, the use of gel is essential to limit the formation of shadow zones, but especially to avoid the presence of air between tissue and probe, which would impair the visibility of the ultrasound image. From the point of view of the mechanical execution, two cases may be distinguished:

- transversal section, in which the probe was oriented with the highlighted point in figure 6.13 toward the mid-line
- longitudinal section, in which the same point was oriented upward, in the direction of the head.

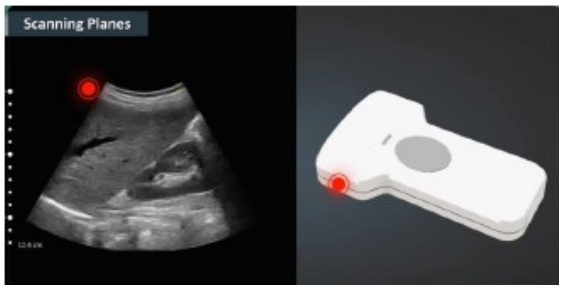

Figure 6.13: *The figure shows the orientation of the scanning probe.*

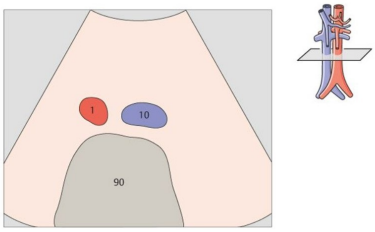

Figure 6.14: *In this figure we can observe the visualization of the transversal section of the IVC [16]*

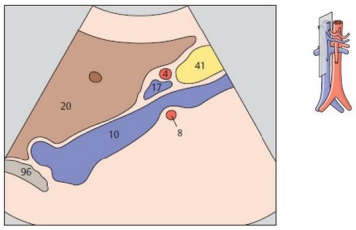

Figure 6.15: *In this figure we can observe the visualization of the longitudinal section of the IVC [16]*

6.8.1 Segmentation software: VIPER

The software is implemented in Matlab and it is an updated version of the algorithm presented in [17] and [18]. The major changes were made to the transverse plane processing algorithm. These allow for varying the median filter size, the dimension of the ROI and contrast modification mode according to the characteristics of the ultrasound video. One of the new features introduced is that in the case where no significant center shift or area change occurs between two consecutive frames, the results obtained for the previous frame are retained. The software still maintains the same result obtained in the previous frame if the area value falls below a certain defined limit. This last control allows the software to continue processing even in cases where the vein tends to close or disappear. The boundary points are identified by evaluating the intensity variation along the segmentation lines, but now a selection of the detected edge points is made and the points considered "wrong" are discarded. In fact, the points too close or too far from the centre of the vein are not considered because anatomically improbable, although vein sizes vary from subject to subject and at different stages of the respiratory/cardiac cycle. Another modification, which also affects the longitudinal plane, involves the

rectangular working portion. This is no longer drawn by the user in the first frame but is estimated based on the input data points and the chosen dimensions. In the longitudinal plane, the segment that cuts the IVC on the left side must no longer be traced [2]. Moreover, the software no longer works in the 2-D Fourier domain to track the two reference points, but performs recognition by Oriented Fast and Rotated BRIEF (ORB) features in each frame. ORBs are descriptors for image detection and matching, which are widely used in computer vision problems [19]. Once the processing of the ultrasound video is completed, the software returns the coordinates of the edge pixels and the processed video with the superimposed segmentation [2]. In particular, for the longitudinal plane it returns the coordinates of the reference points and for the transverse plane it returns the coordinates of the vein center and the value of the segmented area.

Starting from the raw video, through a manual selection of the vein border, was performed an initial segmentation of the inferior vena cava. Initially was selected two high-contrast points, as shown in the figure 6.16, easily visible from the SW throughout the video; then the two edges (upper and lower) of the blood vessel were selected, as shown in figure 6.17. Finally, the last output provided to the software was the right edge of the vein. It represents the boundary of the vein tract to be segmented. Each video has different duration and characteristic, from here

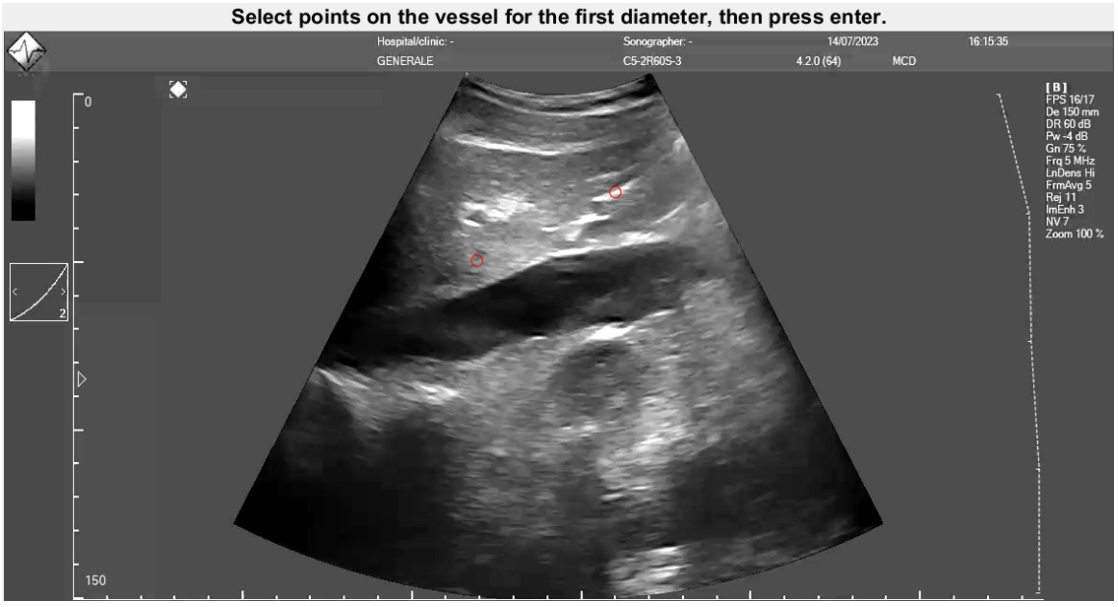

Figure 6.16: *In this figure we can observe the two high-contrast points selected to do the tracking*

the needs to customize two parameters for each elaboration. In fact before starting the segmentation it was set the type of vein (longitudinal or transversal) and the

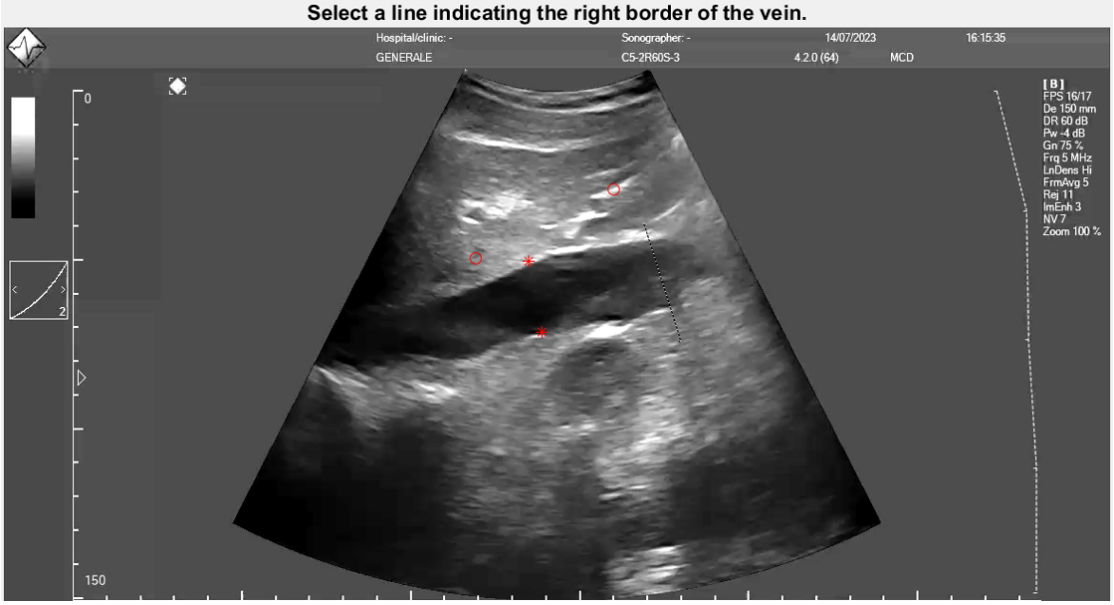

Figure 6.17: *In this figure we can observe the points selected has the edges of the vein*

Start/End frame. This last parameter allow to segment the vein deleting noise or disturb (as tissue overlapping or manual artifact generated by ultrasound probe) obtaining a clean elaboration of the data.

6.8.2 Diameter generator

For a certain number of points, managed by the user, the software VIPER create the diameters, which are distributed along the entire length of the vein. These diameters are obtained from the intersection of a number of lines perpendicular to the mid-line of the vessel, and parallel to each other, with the edges of the vein itself. The diameters return a value in pixels that must be converted to millimeters. This is essential to get practical and accurate feedback on the measurement obtained, so that it can be compared with reference values. Therefore it was evaluated the depth of each single echo-graphic video, that in the specific case was between 90 and 150, after that a different conversion factor was extracted for each depth, and the diameter in pixels was converted to mm. The values of conversion factors obtained ranged from about 0.23 to 0.28.

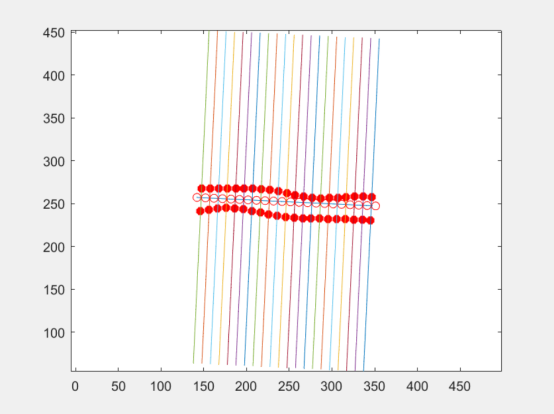

Figure 6.18: *The figure shows the diameters of a video recorded during sweating*

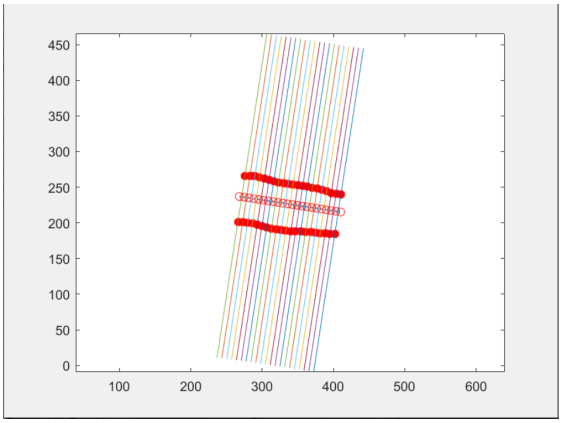

Figure 6.19: *The figure shows the diameters of a video recorded during hydration.*

6.9 Extraction of parameters and normalization

The precise segmentation of blood vessel diameter always has a physiological purpose. So, by extracting the central part of the vein using the software to avoid edge effects, the average value of the diameter of the vena cava was calculated [20]. So all the previous steps , designed to generate a diameter measurement in millimeters from an ultrasound image, are used to calculate physiological indices. Specifically these indices are the collapsibility index (or caval index CI) the respiratory caval index (RCI) and the cardiac caval index (CCI). To obtain these indices from ”mean diameter” it was filtered and treated in this way: ”low-pass filtered, with cut-off frequency equal to mf þ0:5 Hz (Chebyshev of type I, stop band starting at mf + 1:5 Hz, passband from 0 to mf +0:5 Hz)” [20]. In particular, the most interesting parameter from a statistical point of view turned out to be the CI,

which is described by the formula:

$$CI = \frac{D_{max} - D_{min}}{D_{max}} \tag{6.1}$$

It is defined has the collapsibility index and from a physiology point of view is explained has the change in venous flow to the heart due to a change in intra-thoracic pressure. In fact, during spontaneous inspiration, negative intra-thoracic pressure increases venous flow to the heart and reduces the IVC diameter. At end expiration, the intra-thoracic pressure increases to zero, decreasing the venous return and maximizing the IVC diameter. [21]

These measurements were acquired over time, each time an ultrasound measurement was taken, thus: before starting, four times during physical activity, and another four times during hydration.

After the extraction of the parameters, all diameters were normalized in each instant of time with respect to the first value. This approach allows you immediately distinguish the data in the two main phases: hydration and dehydration. In fact, normalization to zero the first value clearly highlights values greater than zero (greater peaks during hydration) and lower values during dehydration. The lowest value is found at the end of the activity. The normalization it was necessary because of high inter-subject variability in vena cava diameter. This makes it possible to make the values comparable to each other.

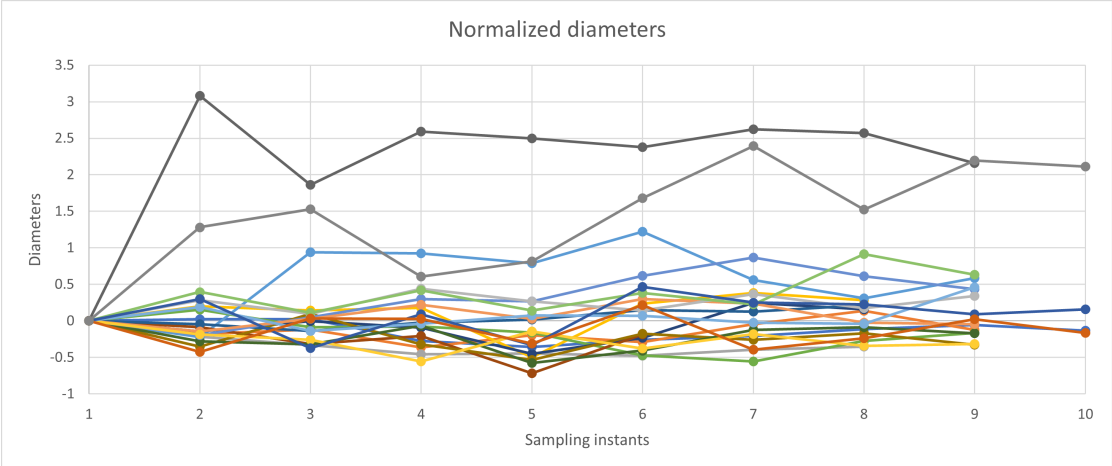

Figure 6.20: *Normalized diameters respect to the first value*

To clarify the general trend and to see if the trend correspond to the initial hypothesis, it was we averaged the diameters of all subjects for each time instant thus obtaining a general trend like that ,shown in figure:

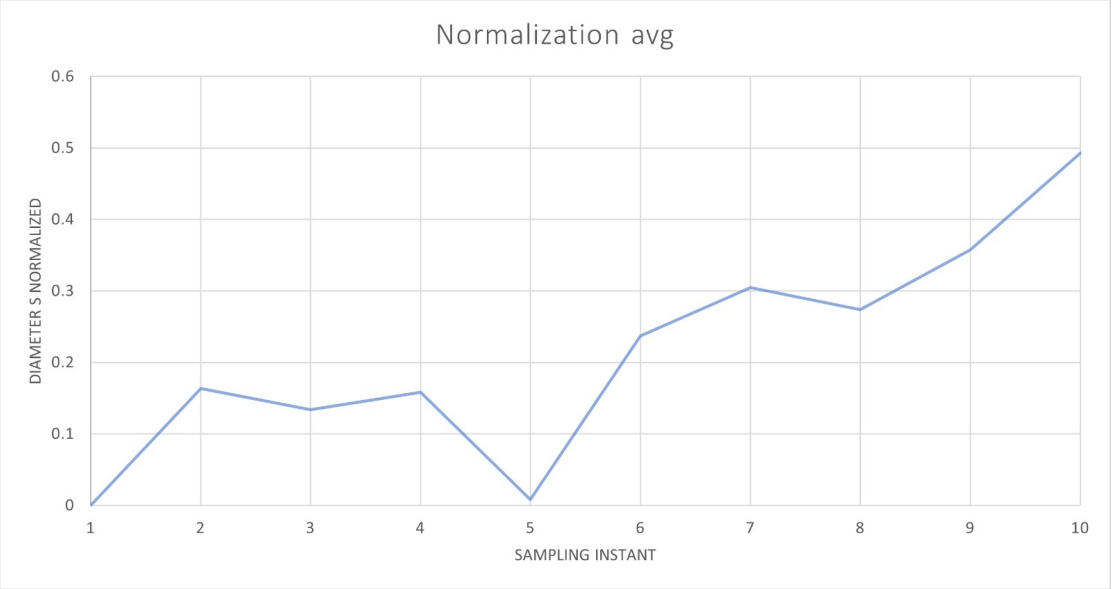

Figure 6.21: *Trend for diameters normalized*

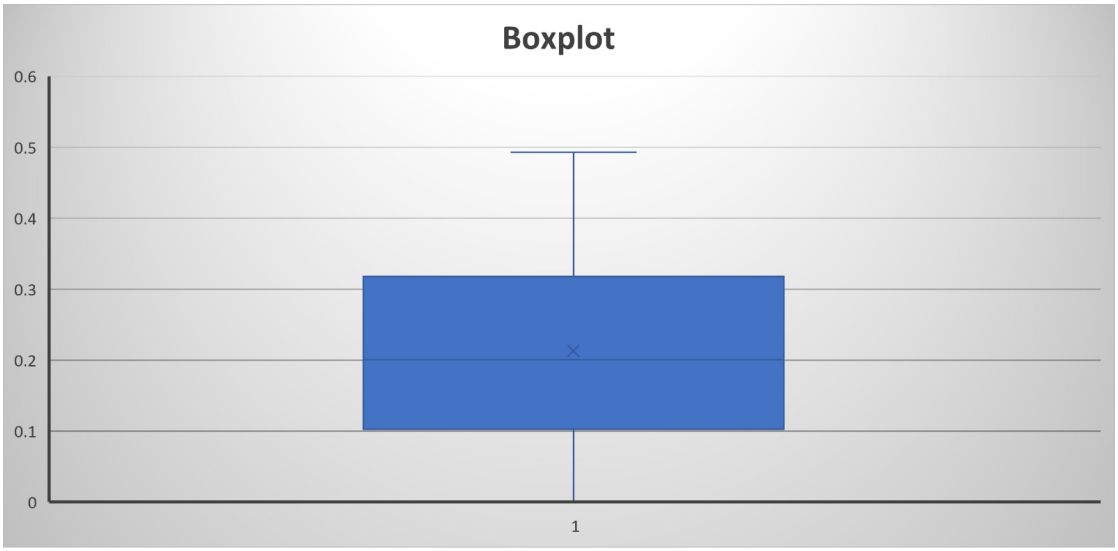

Figure 6.22: *Boxplot for diameters normalized*

Chapter 7

Results

The results confirm the hypothesis that after an exercise activity the diameter of IVC tends to reduce, while after a recovery (hydration) the vein almost return to the initial dimension. Contrary, however, to what we might have thought at the beginning of our project, before we even acquired all the data, we do not have a complete decrease during dehydration and a complete growth during hydration, but they show the trend in figure 7.1. As we can see, during the dehydration phase

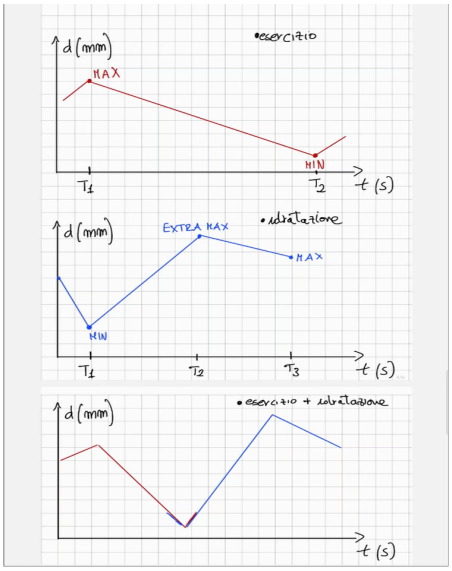

Figure 7.1: *The figure shows the real trend of the IVC diameter. At the top we can see the trend of dehydration, in the middle the trend of hydration and at the bottom the two trends come together.*

some patients need a phase called 'warm up' in which the vein diameter grows to a maximum and then begins to decrease in diameter. Similarly during the hydration

phase the diameter grows to a point above the maximum value found during the dehydration phase and then stabilizes around this value. In general, however, we can say, through the development of a linear model that interpolates the data from the entire data-set averaged, that the trends of the initial assumptions are maintained and that we therefore have a descending phase during dehydration and a growing phase during hydration (as shown in the figure 7.2). However,

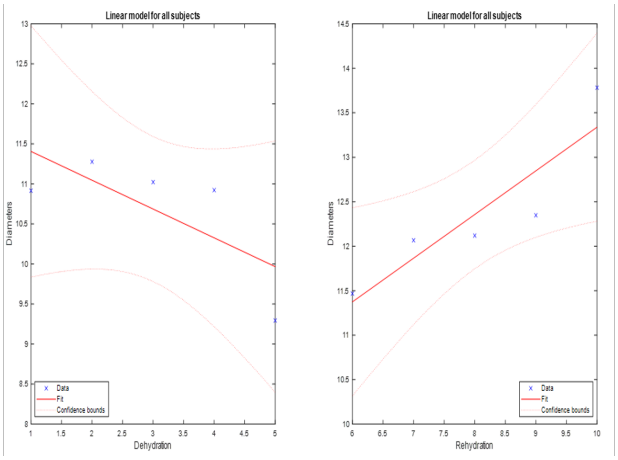

Figure 7.2: *Here are shown the linear model of the entire data-set averaged.*

not all patients in the dataset show the same behavior. In fact, the linear model was applied to each patient, and some of them showed a behavior described as 'peculiar'. As a demonstration, we show in the figure a couple of examples of abnormal behavior:

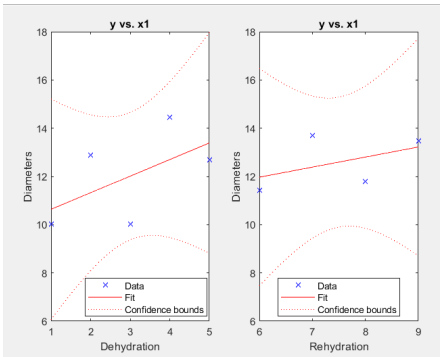

Figure 7.3: *In this figure we can observe a particular behavior for the dehydration phase.*

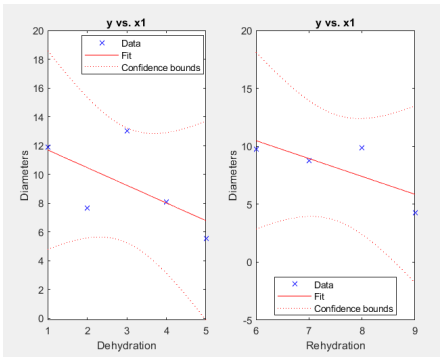

Figure 7.4: *In this figure we can observe a particular behavior for the hydration phase.*

For these subjects defined "particular" the trend was not as expected, and this may be due to various factors, such as physiological behaviors of the vein itself.

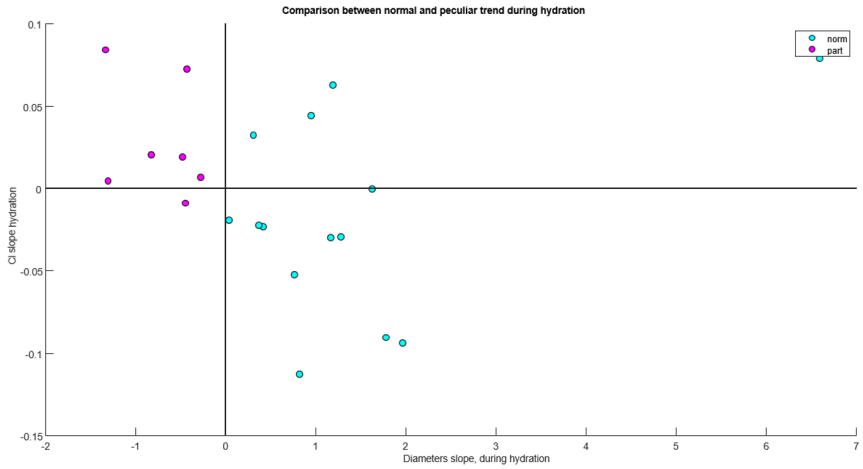

Figure 7.5: *Scatter plot of CI vs Diameter between particular and normal subjects.*

Unfortunately, for statistical purposes, no significant correlations emerged between the candidates called particulars. This may mean that their behavior is subjective and varies based on a multiplicity of factors that may not be observable through our study. But in general once the correlation between these two populations was observed, the spectrum of analysis was broadened focusing on the entire group.

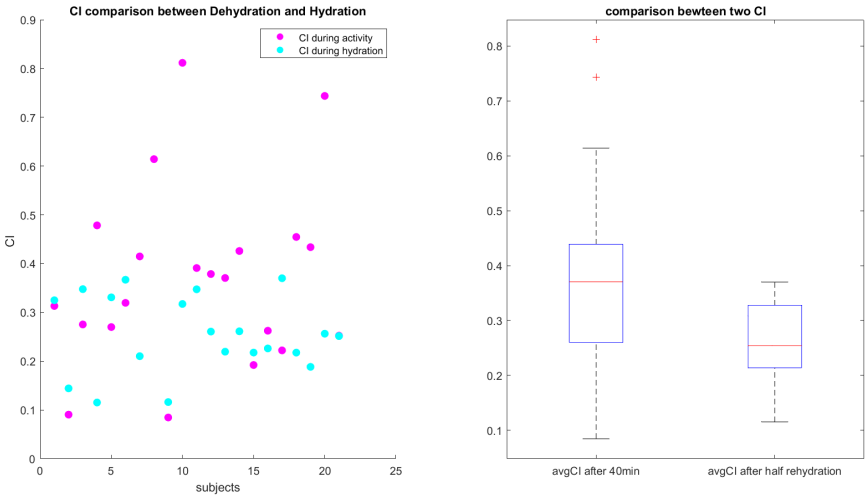

Figure 7.6: *Scatter plot of two different CI for all dataset (L) and boxplot with significance (R)*

The two graphs represent two indicative caval index during the two phases of dehydration and hydration. One of these CI is taken after 40 minutes , when the vein is most empty; while the other measure involve the CI after half hydration, when the highest peak of diameter is measured. Following the statistical significance found among the parameters shown in the graph, the main focus was explored. That is, the presence of differences between sporting and non-sporting subjects was tested.

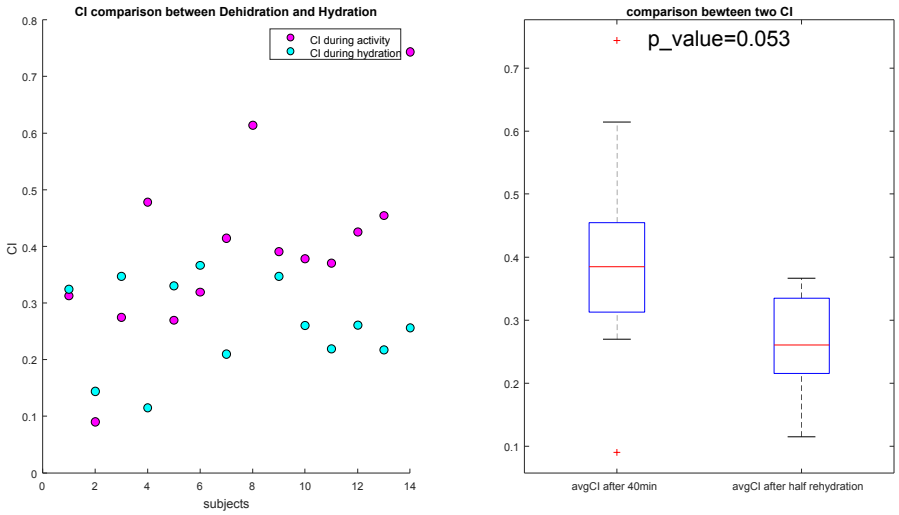

Figure 7.7: *This chart is for the 14 sports subjects. The values of the two CIs are always compared. NB for athletes there is significance between before and after hydration. For non-sportsmen there is no significance and we have not represented them*

A significant result has been achieved. For the category of sports subjects there remains a statistical difference between the analyzed parameters, while for non-sports candidates this difference is not statistically significant.

7.1 Statistical tests

The study of significant parameters to examine the reasons for the decrease and growth of diameter in the two phases were investigated through various statistical tests. To choose which tests to perform, a check on the normality (Gaussian curve) of the variables to be analyzed was carried out by means of 10 tests including Shapiro-Wilk, Shapiro France and Kolmogorov. The result obtained , namely the confirmation of the Gaussian curve for the tested variables led to the use of a parametric statistic and the following tests: Anova, t-test, rankum. The following section will illustrate some tables highlighting the tests performed whether they

are significant or not. The categories tested were different, as noted in the section 7. Firslty the entire dataset, and after the two subgroups: "Athletes" and "Not athletes". In addition it is important emphasize that in accordance with what is observed in the figures 7.3 and 7.4 the test execution involved the two subcategories of subjects particular for hydration phase and dehydration phase.

Test	**Dataset**	**Comparison**	**p_value**	**Signif.**
Ranksum	Sport vs Non Sport	Delta heart rate	0.1352	no
Ranksum	Sport	CI exercise and during hydration	0.0053	yes
Ranksum	Non Sport	CI exercise and during hydration	0.6200	no
Ranksum	Entire dataset	CI exercise and during hydration	0.0110	yes
Ranksum	NormVpartic (dehydr)	Vein empting during effort	0.2006	no
Ranksum	NormVpartic (hydr)	Delta heart rate	0.0858	no
Anova 1	Entire dataset	Avg diam during hydr V Gender	0.1534	no
AnovaN	Entire dataset	Avg diam during hydr V Gender	0.3053	no
AnovaN	Entire dataset	Avg diam during hydration V Age	0.5116	no
AnovaN	Entire dataset	Avg diam during hydration V Sport	0.9661	no
AnovaN	Entire dataset	Avg diam during dehydr V Gender	0.5802	no
AnovaN	Entire dataset	Avg diam during dehydr V Age	0.5423	no
AnovaN	Entire dataset	Avg diam during dehydr V Sport	0.7204	no
t-test2	Sport vs Non Sport	Avg diameter hydration	0.4671	no

Table 7.1: *Test executed*

Legend:

- avg= average
- CI= caval index
- dehydr= dehydration phase
- diam= diameter
- hydr= hydration phase
- Norm= normal
- part= particular

- Signif= significance

In the table above the most relevant tests performed on the various dataset are included. It can be seen that only two tests were significant and have been reported in the 7 section. It is necessary to point out some aspects:

- Delta heart rate is the difference of heart rate between the beginning and end of the effort
- When the caval index comparison appears, we refer to the difference in CI between the end of exercise and about halfway through hydration, when the maximum peak in diameter is witnessed

Chapter 8

Conclusion

At the end of our project we can say that our hypotheses were only partially confirmed. In fact, initially we expected to have a complete decrease during the exercise phase, and thus dehydration, and a complete increase instead during the hydration phase. As shown in the results the trend is more complex although the general trend is in line with the hypothesis made, that is, decrease during dehydration and growth during hydration. The overall normalization, derived from the average of all diameters for each instant, demonstrates this statement well. From the figure 6.21 we can indeed see the initial warm-up phase, the descent to the minimum at the end of the exercise, and the rise during hydration.

In addition to this, the importance of the caval index was confirmed as a key parameter, useful in attesting to diameter variability and making statistically relevant distinctions on the patients under study. This parameter allowed us, in addition to attesting whether the candidates were fluid-deficient, to observe different behavior between athletic and nonathletic subjects. In fact, the vena cava of sports subjects showed greater adaptability to external changes, reacting more quickly to the reintroduction of fluids into the body, more quickly respect to the other subjects.

Certainly this thesis project opens the door to new developments and insights. For example, it would certainly be useful to increase the duration of the exercise phase in order to observe the decreasing trend in this phase even more surely. The use of a more uniform candidate dataset could also contribute to the further improvement of the results and could give rise to new significances that, with a heterogeneous dataset such as the one in this thesis project, did not arise from the analyses performed.

Bibliography

[1] G.C. Balboni; A. Bastianini; E. Brizzi; L. Comparini; G. Filogamo; P. Fusaroli; G. Giordano-Lanza; C.E. Grossi; F.A. Manzoli; G. Marinozzi; A. Miani; P. Motta; E. Nesci; G.E. Orlandini; A. Passaponti; E. Reale; A. Ruggeri; A. Santoro; D. Zacchero. *Anatomia Umana I.* Milano, MI: edi-ermes, 1984 (cit. on pp. 3, 4, 7, 8).

[2] Aurora Giambartolomei; Michela Pieragostini. «Test of a new ulstrasound system for monitoring the edges of the inferior vena cava». MA thesis. Torino: Politecnico di Torino, 2023 (cit. on pp. 4, 5, 8, 11, 23, 41).

[3] G. Losano; R. Rastaldo; P. Pagliaro; A. Chiribiri. *Fisiologia cardiovascolare.* River publisher, 2013 (cit. on p. 4).

[4] Mesin L.; Albani S.; Policastro P.; Pasquero P.; Porta M.; Melchiorri C.; Leonardi G.; Albera C.; Scacciatella P.; Pellicori P.; Stolfo D.; Grillo A.; Fabris B.; Bini R.; Giannoni A.; Pepe A.; Ermini L.; Seddone S.; Sinagra G.; Antonini-Canterin F.; Roatta S. «Assessment of phasic changes of vascular size by automated edge tracking-state of the art and clinical perspectives». In: *Frontiers in Cardiovascular* 8 (Jan. 2022) (cit. on pp. 5, 6).

[5] Cindy L. Stanfield. *Principles of human physiology - IV edition.* Pearson/Benjamin Cummings, 2011 (cit. on pp. 9, 12).

[6] G.C. Balboni; A. Bastianini; E. Brizzi; L. Comparini; G. Filogamo; P. Fusaroli; G. Giordano-Lanza; C.E. Grossi; F.A. Manzoli; G. Marinozzi; A. Miani; P. Motta; E. Nesci; G.E. Orlandini; A. Passaponti; E. Reale; A. Ruggeri; A. Santoro; D. Zacchero. *Anatomia Umana II.* Milano, MI: edi-ermes, 1984 (cit. on pp. 9, 10).

[7] Bojan Knap. «Hydration and Physical Activity». In: *Res Inves Sports Med* 7(4) (Apr. 2021) (cit. on pp. 29, 30).

[8] Andrea Poli; Francesco Visoli. «Idratazione e salute». In: *Rivista della Società Italiana di Medicina Generale* 3 (2009) (cit. on p. 29).

[9] Anna L. Waterbrook; Amish Shah; Elisabeth Jannicky; Uwe Stolz; Randy P. Cohen; Austin Gross; Srikar Adhikari. «Status in College Football Players During Preseason Camp». In: *J Ultrasound Med* 34 (2015), pp. 239–245 (cit. on pp. 29, 30).

[10] Samuel N. Cheuvront; Michael N. Sawka. «Hydration Assessment of Athletes». In: *Sports Science Exchange* 18(2) (2005) (cit. on p. 30).

[11] Daniele Orso; Nicola Guglielmo; Nicola Federici; Francesco Cugini; Alessio Ban; Filippo Mearelli; Roberto Copetti. «Accuracy of the caval index and the expiratory diameter of the inferior vena cava for the diagnosis of dehydration in elderly». In: *J Ultrasound* (2016) (cit. on p. 31).

[12] URL: `https://www.medicalexpo.it/prod/telemed-medical-systems/product-70298-718259.html` (cit. on p. 34).

[13] *Tanita BC-730 Scale*. Tanita (cit. on p. 36).

[14] *Polar H10 Heart Rate Sensor*. Polar (cit. on p. 36).

[15] Mesin L.; Giovinazzo T.; D'Alessandro S.; Roatta S.; Raviolo A.; Chiacchiarini F.; Porta M.; Pasquero P. «Improved repeatability of the estimation of pulsatility of inferior vena cava». In: *Ultrasound in Medicine Biology* 45 (10 2019), pp. 2830–2843 (cit. on p. 38).

[16] URL: `https://radiologykey.com/vessels/` (cit. on p. 40).

[17] Mesin L.; Pasquero P.; Roatta S. «Tracking and monitoring pulsatility of a portion of inferior vena cava from ultrasound imaging in long axis». In: *Ultrasound in Medicine Biology* 45 (5 2019), pp. 1338–1343 (cit. on p. 40).

[18] Mesin L.; Pasquero P.; Roatta S. «Multi-directional Assessment of Respiratory and Cardiac Pulsatility of the Inferior Vena Cava From Ultrasound Imaging in Short Axis». In: *Ultrasound in Medicine Biology* 46 (12 2020), pp. 3475–3482 (cit. on p. 40).

[19] Rublee E.; Rabaud V.; Konolige Gary Bradski K. «ORB: an efficient alternative to SIFT or SURF». In: *International Conference on Computer Vision* (2011) (cit. on p. 41).

[20] Ermini L.; Seddone S.; Policastro P.;Mesin L.; Pasquero P.; Roatta S. «The cardiac caval index: improving noninvasive assessment of cardiac preload.» In: *Journal of Ultrasound in Medicine* 41 (9 2022), pp. 2247–2258 (cit. on p. 43).

[21] Matthew J. Kaptein; Elaine M. Kaptein. «Inferior Vena Cava Collapsibility Index: Clinical Validation and Application for Assessment of Relative Intravascular Volume». In: *AKDH* 28 (3 2021), pp. 218–226 (cit. on p. 44).